5 **Yamagami H, Matsumoto T, Fujiwara N *et al.*** Trehalose 6,6'-dimycolate (cord factor) of Mycobacterium tuberculosis induces foreign-body- and hypersensitivity-type granulomas in mice. *Infect Immun* 2001; **69**: 810–5

6 **Strohmeier GR, Fenton MJ.** Roles of lipoarabinomannan in the pathogenesis of tuberculosis. *Microbes Infect* 1999; **1**: 709–17

7 **Underhill DM, Ozinsky A, Hajjar AM *et al.*** The Toll-like receptor 2 is recruited to macrophage phagosomes and discriminates between pathogens. *Nature* 1999; **401**: 811–5

8 **Means TK, Lien E, Yoshimura A, Wang S, Golenbock DT, Fenton MJ.** The CD14 ligands lipoarabinomannan and lipopolysaccharide differ in their requirement for Toll-like receptors. *J Immunol* 1999; **163**: 6748–55

9 **Means TK, Wang S, Lien E, Yoshimura A, Golenbock DT, Fenton MJ.** Human toll-like receptors mediate cellular activation by Mycobacterium tuberculosis. *J Immunol* 1999; **163**: 3920–7

10 **Sendide K, Reiner NE, Lee JS, Bourgoin S, Talal A, Hmama Z.** Cross-talk between CD14 and complement receptor 3 promotes phagocytosis of mycobacteria: regulation by phosphatidylinositol 3-kinase and cytohesin-1. *J Immunol* 2005; **174**: 4210–9

11 **Chin JL, Kadhim SA, Batislam E *et al.*** Mycobacterium cell wall: an alternative to intravesical bacillus Calmette Guerin (BCG) therapy in orthotopic murine bladder cancer. *J Urol* 1996; **156**: 1189–93

12 **Brennan PJ, Nikaido H.** The envelope of mycobacteria. *Annu Rev Biochem* 1995; **64**: 29–63

13 **Chatterjee D.** The mycobacterial cell wall: structure, biosynthesis and sites of drug action. *Curr Opin Chem Biol* 1997; **1**: 579–88

14 **Khalil IA, Kogure K, Futaki S *et al.*** Octaarginine-modified multifunctional envelope-type nanoparticles for gene delivery. *Gene Ther* 2007; **14**: 682–9

15 **Kogure K, Moriguchi R, Sasaki K, Ueno M, Futaki S, Harashima H.** Development of a non-viral multifunctional envelope-type nano device by a novel lipid film hydration method. *J Control Release* 2004; **98**: 317–23

16 **Khalil IA, Kogure K, Futaki S, Harashima H.** High density of octaarginine stimulates macropinocytosis leading to efficient intracellular trafficking for gene expression. *J Biol Chem* 2006; **281**: 3544–51

17 **Moriguchi R, Kogure K, Akita H *et al.*** A multifunctional envelope-type nano device for novel gene delivery of siRNA plasmids. *Int J Pharm* 2005; **301**: 277–85

18 **Akaza H, Iwasaki A, Ohtani M *et al.*** Expression of antitumor response. Role of attachment and viability of bacillus Calmette-Guérin to bladder cancer cells. *Cancer* 1993; **72**: 558–63

19 **Iwasaki A, Kawai K, Hayashi H *et al.*** Immunological protection induced by bacillus Calmette-Guérin treatment in a murine bladder tumor model. *Int J Urol* 2002; **9**: 219–24

20 **Futaki S, Ohashi W, Suzuki T *et al.*** Stearylated arginine-rich peptides: a new class of transfection systems. *Bioconjug Chem* 2001; **12**: 1005–11

21 **Homhuan A, Kogure K, Akaza H *et al.*** New packaging method of mycobacterial cell wall using octaarginine-modified liposomes: enhanced uptake by and immunostimulatory activity of dendritic cells. *J Control Release* 2007; **120**: 60–9

22 **Beatty WL, Rhoades ER, Ullrich HJ, Chatterjee D, Heuser JE, Russell DG.** Trafficking and release of mycobacterial lipids from infected macrophages. *Traffic* 2000; **1**: 235–47

23 **Watanabe Y, Watari E, Matsunaga I *et al.*** BCG vaccine elicits both T-cell mediated and humoral immune responses directed against mycobacterial lipid components. *Vaccine* 2006; **24**: 5700–7

24 **Azuma I, Ribi EE, Meyer TJ, Zbar B.** Biologically active components from mycobacterial cell walls. I. Isolation and composition of cell wall skeleton and component P3. *J Natl Cancer Inst* 1974; **52**: 95–101

25 **Vermorken JB, Claessen AM, van Tinteren H *et al.*** Active specific immunotherapy for stage II and stage III human colon cancer: a randomised trial. *Lancet* 1999; **353**: 345–50

26 **Yamamura Y, Azuma I, Taniyama T *et al.*** Immunotherapy of cancer with cell wall skeleton of *Myocobacterium bovis*-Bacillus Calmette-Guerin: experimental and clinical results. *Ann NY Acad Sci* 1976; **277**: 209–27

27 **Mudhakir D, Akita H, Khalil IA, Futaki S, Harashima H.** Pharmacokinetic analysis of the tissue distribution of octaarginine modified liposomes in mice. *Drug Metab Pharmacokinet* 2005; **20**: 275–81

28 **Hosotani R, Miyamoto Y, Fujimoto K *et al.*** Trojan p16 peptide suppresses pancreatic cancer growth and prolongs survival in mice. *Clin Cancer Res* 2002; **8**: 1271–6

29 **Miyazaki J, Kawai K, Oikawa T *et al.*** Uroepithelial cells can directly respond to *Mycobacterium bovis* bacillus Calmette-Guerin through Toll-like receptor signalling. *BJU Int* 2006; **97**: 860–4

30 **Ikeda N, Toida I, Iwasaki A, Kawai K, Akaza H.** Surface antigen expression on bladder tumor cells induced by bacillus Calmette-Guerin (BCG): a role of BCG internalization into tumor cells. *Int J Urol* 2002; **9**: 29–35

Correspondence: Akira Joraku, Graduate School of Comprehensive Human Sciences, Department of Urology, University of Tsukuba, 1-1-1 Tennodai, Tsukuba, Ibaraki 305-8575, Japan.
e-mail: ajoraku@md.tsukuba.ac.jp

Abbreviations: **CW**, cell wall; **R8-liposomes**, octaarginine-modified liposomes; **FTSC**, fluorescein-5-thiosemicarbazide; **STR-R8**, stearylated-octaarginine; **CWS**, cell wall skeleton; **TLR**, Toll-like receptor.

Tsukasa Seya
Misako Matsumoto
Takashi Ebihara
Hiroyuki Oshiumi

Functional evolution of the TICAM-1 pathway for extrinsic RNA sensing

Authors' address
Tsukasa Seya[1], Misako Matsumoto[1], Takashi Ebihara[1], Hiroyuki Oshiumi[1]
[1]Department of Microbiology and Immunology, Hokkaido University Graduate School of Medicine, Sapporo, Japan.

Correspondence to:
Tsukasa Seya
Department of Microbiology and Immunology
Hokkaido University Graduate School of Medicine
Kita 15, Nishi 7, Kita-ku
Sapporo 060-8638
Japan
Tel.: +81 11 706 5073
Fax: +81 11 706 7866
e-mail: seya-tu@pop.med.hokudai.ac.jp

Acknowledgements
We thank Drs A. Matsuo, T. Tsujita, A. Ishii, M. Shingai, M. Sasai, and K. Funami in our laboratory for their valuable discussions. This work was supported in part by CREST, JST (Japan Science and Technology Corporation), and by Grants-in-Aid from the Ministry of Education, Science, and Culture (Specified Project for Advanced Research) and the Ministry of Health, Labor, and Welfare of Japan, and by the Takeda Science Foundation, Uehara memorial Foundation, Noruhtec Foundation, Akiyama Foundation and Mitsubishi Foundation. Financial supports by the Sapporo Biocluster 'Bio-S' the Knowledge Cluster Initiative of the MEXT, and the Program of Founding Research Centers for Emerging and Reemerging Infectious Diseases, MEXT are gratefully acknowledged.

Immunological Reviews 2009
Vol. 227: 44–53

Immunological Reviews
0105-2896

Summary: The type I interferon (IFN) is a host defense factor against microbial pathogens in vertebrates. In mammals, retinoic acid-inducible gene I (RIG-I) and melanoma differentiation-associated gene 5 (MDA5) in the cytoplasm are regarded as sensors for double-stranded RNA (dsRNA) and trigger IFN regulatory factor-3 (IRF-3) activation followed by type I IFN induction through the mitochondrial antiviral signaling (MAVS) adapter. This intrinsic pathway appears to link the main protective responses against RNA virus infection in mammals. On the other hand, human Toll-like receptor 3 (TLR3) is localized in the endosomal membrane or cell surface and signals the presence of extrinsic dsRNA. In response to RNA stimulation, TLR3 recruits the Toll-interleukin 1 receptor domain (TIR)-containing adapter molecule 1 (TICAM-1) adapter and induces IRF-3 activation followed by IFN-β promoter activation. Human TLR3 is localized limitedly extent in myeloid dendritic cells, fibroblasts, and epithelial cells. The TICAM-1 and cytoplasmic MAVS pathways converge at the IRF-3-activating kinase in human cells. The reason for the involvement of this extrinsic mode of IFN-inducing pathways in the dsRNA response remains unknown. In fish, two TLRs, i.e. endoplasmic TLR3 and cell surface TLR22, participate in teleost IFN production without the activation of IRF-3. TLR22 is distinct from mammalian TLR3 in terms of cellular localization, ligand selection, and tissue distribution. TLR22 may be a functional substitute for human cell surface TLR3 and may serve as a surveillance molecule for detecting dsRNA virus infection and alerting the immune system for antiviral protection in fish. In this review, we discuss the fundamentals of the extrinsic dsRNA recognition system, which has evolved to induce cellular effectors to cope with dsRNA virus infection across different vertebrate species.

Keywords: Toll-like receptor, evolution, dsRNA recognition, TICAM-1 (TRIF)

Introduction

Invading pathogens express specific pattern molecules and are recognized by host pattern recognition receptors (PRRs) (1, 2), representatives of which are Toll-like receptors (TLRs), Nod-like receptors (NLRs), and RNA helicases [retinoic acid-inducible gene I (RIG-I), melanoma differentiation-associated protein 5 (MDA5), etc.]. These receptors signal the presence of microbial patterns in myeloid dendritic cells (mDCs) and thus induce potent activation of the systemic host defense response (3). Recent studies on pattern receptors of

the innate immune system have increased our understanding of how mDCs mature through infection and subsequently orchestrate cellular immunity (4, 5). These molecules also serve as adjuvants for the induction of antigen-specific acquired immunity. TLRs, RIG-I-like helicases (RLHs), and NLRs are major targets for investigating the induction of robust acquired immune responses upon pathogen stimulation. These studies have been conducted using gene-disrupted mice and in *in vitro* human systems.

It has been reported that human cells induce interferon-β (IFN-β) in response to various RNA structures (6, 7). Double-stranded RNA (dsRNA) and its analog polyinosinic–polycytidylic acid (polyI:C) have been identified as potent immune stimulators of viral patterns and are recognized by PRRs. PRRs link cytoplasmic adapter molecules in these mammalian cells. Cytoplasmic RLH and membrane-associated TLRs that induce IFN-α/β involve the mitochondrial antiviral signaling (MAVS) (also known as IPS-1, Cardif, or VISA) or TICAM-1 [Toll-interleukin-1 receptor (IL-1R) (TIR) domain-containing adapter-inducing IFN-β (TRIF)] adapters, respectively, to converge the signal at IRF-3-activating kinases for IFN-β induction (4, 5, 8). IFN-β induction is IRF-3 dependent in mDCs and fibroblasts/epithelial cells (4, 5). By contrast, IFN-α/β is differentially induced in an IRF-7-dependent manner in plasmacytoid DCs (pDCs) (9). This allows activation of the myeloid differentiation factor 88 (MyD88) adapter protein and IKKα [inhibitor of nuclear factor (NF) κB (IκB) kinase α] kinase, which directly activates the IRF-7 transcription factor (10). However, the molecular assembly and mechanism involved in polyI:C-mediated activation of transcription factors still remain unclear in mice and humans.

Some PRRs preferentially recognize nucleic acid structures that are unique to infectious microbes. Type I IFN induction and cytotoxic T-lymphocyte (CTL)/natural killer (NK) cell activation are major outputs for RNA-sensing PRRs in mammalian cells (5, 11). A variety of RNA sensors in the cytoplasm or membranes are engaged in the detection of microbial RNA. These are expressed in a cell-type specific fashion and participate in IFN-α/β production in various cell types. However, the combinations of these receptors that induce cellular immunity still remain undetermined. It is generally accepted that RNA patterns that are exogenously provided or are produced in bystander cells are internalized by mDCs through phagocytosis and are then recognized by endosomal PRRs. By contrast, RNA patterns produced in the cytoplasm of infected cells are directly recognized by PRRs present in the cytoplasm (12). In this review, we adopted an evolutional approach to study TLRs present on the cell membrane and the recognition of the external dsRNA pattern that is specifically formed in other cells during virus replication.

Fish (teleost) have >20 TLRs that include orthologs of human TLRs and other TLRs unique to lower vertebrates living in water (13, 14). Teleost have orthologs of the IFN-inducing genes of mammals and PRRs for microbial pattern recognition. Teleost also have a TICAM-1 ortholog which has no TRAF-binding site but retains the RIP1-binding site (15, 16). Fish may have orthologs of RLH and NLRs. Hence, by comparing the mammalian PRR receptor/adapter system with that of fish, it is possible to examine the development of the innate recognition system during evolution. Molecular evolution by which the mammalian immune system has been established in the current form can be analyzed through the genomic information of vertebrate TLR systems. In this study, we cast insight into the functional properties of fish TLRs and adapters involved in IFN induction.

Recognition of RNA duplexes in vertebrates

Viral replication usually generates dsRNA in the cytoplasm of infected cells and signals to activate antiviral responses. dsRNA, stem-loop structure of RNA, 5′-uncapped triphosphate of RNA, and specific RNA sequences are rapidly recognized by PRRs in the cytoplasm (4, 5, 17), then implicated in host defense (Fig. 1). Many pattern-sensing receptors have been identified in mammals: PKR (dsRNA-dependent protein kinase), Dicer of the short interfering/microRNA system, RLHs including RIG-I, MDA5, and LGP2, and other helicases. These receptors are accompanied by adapters that transduce the dsRNA-sensing signal downstream. Other RNA-sensing molecules such as helicases may also be present in the cytoplasm to join a molecular assembly for foreign RNA detection. The synthesized dsRNAs are incorporated into these molecular complexes to prohibit RNA replication in virus-infected cells.

TLR3 is present in the early endosome and can recognize dsRNA delivered inside the endosomal membrane (18). TLR3 may not have a direct role in capturing dsRNA generated by virus replication in the cytoplasm, but it has an important role in trapping phagocytosed dsRNA (Fig. 2), which is usually wrapped in a membrane that originates from the infected cell (19). In comparison to the direct recognition system of dsRNA in the cytoplasm, this mode of RNA recognition is unique and sophisticated, concerning activation of cellular immunity. As RNA-sensing TLRs and RLH are conserved across vertebrates (20), we hypothesize

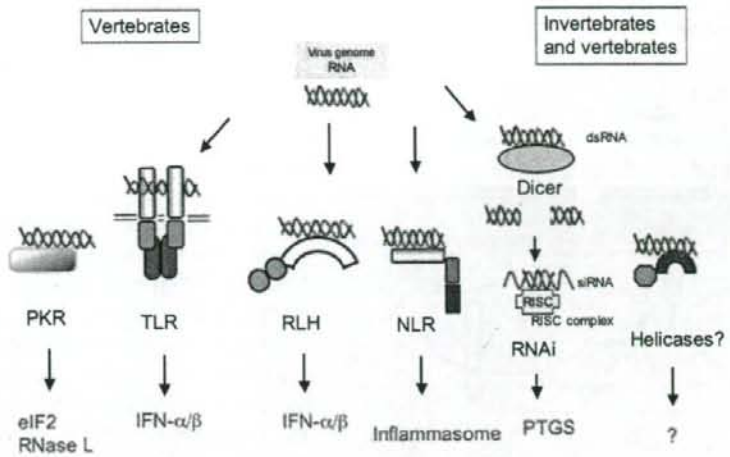

Fig. 1. Various RNA sensors in vertebrates. dsRNA are generated during virus replication. Major RNA sensors in vertebrate cells and their responses on stimulation with dsRNA are indicated. Dicer and RNA-recognizing helicases work even in invertebrates. How dsRNA selects a variety of RNA pattern sensors remains largely unknown. PTGS, post-transcriptional gene silencing.

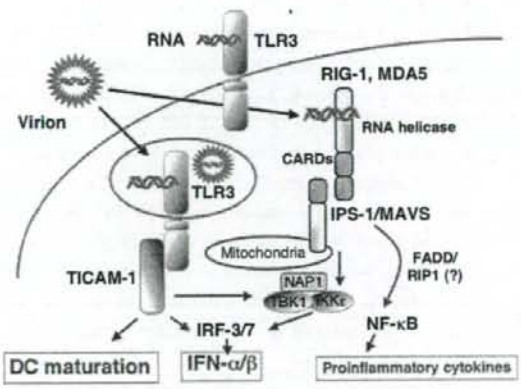

Fig. 2. Cell surface, endosomal and cytoplasmic recognition of dsRNA in mammalian cells. TLR3 is distributed either on the cell surface or in the endosome. Its distribution ratio depends on cell types. RLH (RIG-I and MDA5) reside in the cytoplasm. Adapter molecules, TICAM-1 and MAVS, are localized in the cytoplasm. Upon stimulation, TLR3 recruits TICAM-1 near the endosomal membrane, while MAVS recruits RLH on the mitochondrial membrane. The known outputs of TLR3 and RLH are indicated by red. TLR, Toll-like receptor; RIG, retinoic acid-inducible gene; RLH, RIG-I-like helicase; TICAM, Toll-interleukin 1 receptor domain-containing adapter molecule.

that the two distinct pathways of dsRNA recognition were established in a vertebrate ancestor ~500 Ma and that the two systems have been preserved in mammals (Fig. 2). We focus on the fish membrane-associated dsRNA recognition system and analyze it in terms of its physiological significance and functional feature and also from an evolutionary point of view. We also address the question of why vertebrates need the surface system for dsRNA recognition in addition to the cytoplasmic virus-sensing systems.

Surface recognition of dsRNA in mammals

We initiated a study on the functions of the membrane-associated dsRNA recognition receptor TLR3 in human cells. Stimulation of human fibroblasts/epithelial cells with polyI:C leads to the production of type I IFN. We have produced monoclonal antibodies (mAbs) against human TLR3 and obtained one which blocks polyI:C binding to TLR3, named the mAb TLR3.7 (21). The TLR3.7 mAb interferes with IFN-β production induced by exogenously added polyI:C in human fibroblasts/epithelial cells (18, 21). Hence, it appears that TLR3.7 mAb blocks the interaction between TLR3 and polyI:C on the cell surface by binding to TLR3. If this is the case, human TLR3 must be localized on the cell surface of the fibroblast to capture external dsRNA. This hypothesis was proven by results from fluorescence-assisted cell sorting (FACS) and imaging analyses (Fig. 3*A*). However, using the same mAb, human mDC TLR3 could not be detected on the surface (18) but was found to be localized in intracellular compartments, particularly endosome (Fig. 3*A*). mDCs respond to polyI:C to induce type I IFN in the early endosome (22, 23). In this case, how does endosomal TLR3 recognize polyI:C outside the cells? It is rational that there is a transporter that shuttles dsRNA from the cell surface to the endosome in mammals (5). The recognition of dsRNA by TLR3 on the cell surface is

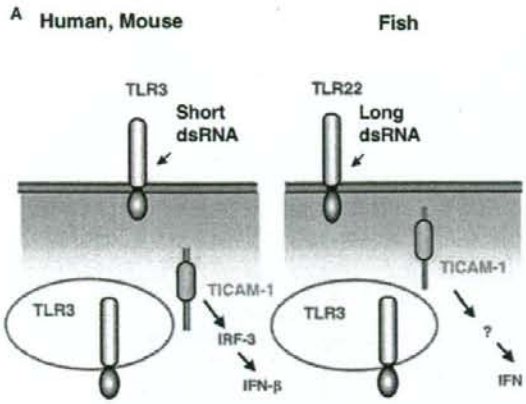

B **IFN-inducing receptors in human and fish**

Genes	Human	Fish
TLR3	+	+
RIG-I	+	–
TLR22	–	+
IFN	+	+

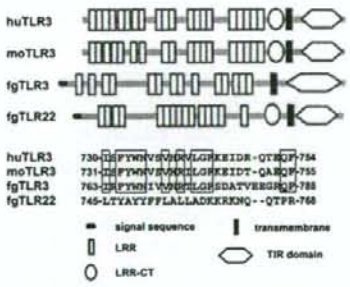

Fig. 3. Different TLRs cover surface dsRNA recognition in fish and mammals. (A) TLR3 and TLR22 in vertebrates. In human and mouse, TLR3 encompasses cell surface and endosomal RNA sensing and induces IRF-3 activation. In fish, two distinct gene products, TLR3 and TLR22, participate in dsRNA sensing. IFN is induced in an IRF-3-independent fashion. Although the structural information is not shown in the panel, mammalian TICAM-1 structurally differs from fish TICAM-1. IRF-3-activating kinase indirectly assembles in an N-terminal portion of mammalian TICAM-1 but not fish TICAM-1. A C-terminal portion contributes to IFN promoter activation in fish cells. (B). Difference of IFN-inducing receptors between human and fish. Upper table indicates that humans lack TLR22 while fish lack RIG-I, although both have IFN-inducible pathways. The structural differences among human (hu) TLR3, mouse (mo) TLR3, fgTLR3, and fgTLR22 are depicted in the lower panel. The primary structures of the linker region (a determinant of TLR3 localization) are shown below the structural models.

experimentally proven by using the mAb probe for determining the localization of human TLR3. However, the dsRNA shuttling system has not yet been proved.

If TLR3 participates in the induction of IFN-β in epithelial cells, its downstream molecules should activate IRF-3. Therefore, we searched for an adapter molecule that could directly interact with TLR3 and activate IRF-3; the molecule was identified by employing the yeast two-hybrid system. It was named TICAM-1 (24) and is now popularly known as TRIF (25).

Human TICAM-1 consists of an N-terminal region (1–234), a TIR domain (235–500), and a C-terminal region (501–680). The N-terminal region of TICAM-1 harbors tumor necrosis factor (TNF) receptor-associated factor (TRAF) family proteins (26, 27) and forms a complex containing IRF-3-activating kinases (28, 29). This kinase complex is crucial for activating the IFN-β promoter (28, 29) and inducing the activation of NK (5, 30) and CTL (12, 31) effector cells (Fig. 4). The C-terminal region of TICAM-1 can recruit receptor-interacting protein-1 (RIP-1), and this event is followed by the activation of other effectors (32). All these signaling events constitute the TICAM-1 pathway. Human and mouse TICAM-1 pathways involve mDC maturation, cytokine/chemokine induction, cross-presentation of exogenous antigens for proliferation of $CD8^+$ T cells (5, 12, 31, 33), NK cell activation (30, 34), and induction of autophagy and apoptosis (35). CD4+ regulatory T (Treg) cells and Th17 cells may be induced by mDCs matured through TICAM-1 signaling. TICAM-1 may act as a platform that recruits various signaling molecules for mDC output in mammals. However, one question that remains unanswered is whether the TICAM-1 pathway is conserved in lower vertebrates such as fish.

Surface recognition of dsRNA in fish

Fish [*Takifugu rubripes* (fg)] have ~20 TLRs and three TLR adapters, i.e. fgMyD88, fgTICAM-1, and fgTIRAP/Mal (36). By using the yeast two-hybrid analysis system, we found at least two TLRs that share the fgTICAM-1 adapter (37). The first report on fgTLRs (13) showed that fgTLR3 and fgTLR22 choose the fgTICAM-1 adapter in fish cells and induce fish type I IFN by recognizing dsRNA. fgTLR3 and fgTLR22 are quite different in their primary structures (Fig. 3B) and are classified into different clades by gene tree analysis (13, 37). However, both fgTLR3 and fgTLR22 directly bind to fgTICAM-1 in fish cells as well as in yeast. Confocal analysis has shown that fgTLR3 resides in the endoplasmic reticulum (ER) and recognizes relatively short dsRNA, whereas fgTLR22 recognizes long dsRNA present on the cell surface (37). The

properties of fgTLR3 and fgTLR22 are summarized in Fig. 3B. fgTLR22 is particular, as fgTLR22 preferentially recognizes long dsRNA, localizes exclusively to the cell surface, and is widely distributed across tissue/organs. In summary, two of the receptors that recognize dsRNA are also involved in the TICAM-1 pathway in fish. The fish TICAM-1 pathway leads to the activation of the IFN promoter.

The next question is how TICAM-1 is assembled by TLR22 to transmit the dsRNA recognition signal. Possible answers may lie in the structural difference between mammalian and teleost TICAM-1 (Fig. 3B). Over-expression of zebrafish (zf)TICAM-1 activates the zfIFN promoter, but zfTICAM-1 does not interact with zfTRAF6 (16). Results from genomic retrieval analysis suggest that zebrafish lacks IRF-3. The zfTICAM-1 N-terminal region does not contain the TRAF6-binding motif (that participates in IRF-3 activation), and the C-terminal region of zfTICAM-1 can adequately activate the zfIFN promoter. This observation suggests the involvement of RIP1-mediated NF-κB activation in zfIFN promoter activation (16, 37).

Human TICAM-1 stimulates IRF-3-mediated type I IFN induction by means of its N-terminal region (38, 39) (Fig. 4). Thus, fish TICAM-1 behaves like human TICAM-1; however, fish TICAM-1 does not employ IRF-3 to activate the IFN-β promoter (16, 40). Although the TICAM-1 pathway is conserved across both fish and humans, the molecular bases for IFN induction in response to extrinsic dsRNA differ in the two vertebrate species (Fig. 3). Our speculation is that although fish cells have an IFN output similar to that of human cells, the signal cascade that leads to IFN production is modally different. Teleost TICAM-1, which is structurally dissimilar to human TICAM-1 (36), might help in explaining the differential selection of the signal pathways.

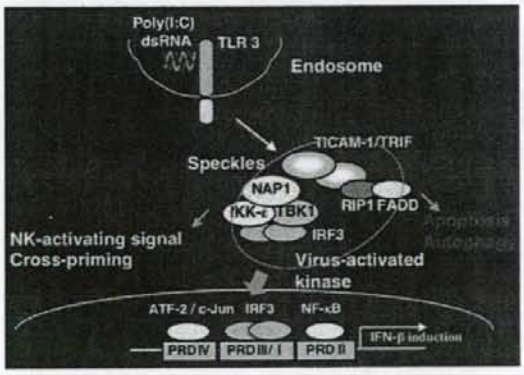

Fig. 4. TICAM-1 is dissociated from TLR3 to form a signaling unit, Speckle. In human cells, TICAM-1 once detached from TLR3 serves as a signaling platform to induce apoptosis, autophagy, NK activation, and cross-priming. TICAM-1 undergoes some modification secondary to complex formation with TLR3 and dissociated from TLR3 with unknown mechanism. The pathways for NK activation, CTL induction, and autophagy are not yet identified, although the pathway for apoptosis is getting clarified. It is undetermined whether surface-expressed TLR3 or TLR22 retain the cellular responses.

How does human TLR3 substitute for TLR22 in mammals?

The differences between TLR22 and TLR3 can be summarized as follows. Based on confocal microscopy and FACS analyses, over-expressed fgTLR22 is localized on the cell surface, while fgTLR3 resides in the ER and endosomes in fish cells (37). fgTLR22 is ubiquitously distributed over the organs/tissues of teleost, while human and fgTLR3 are present only in a limited cell repertoire. These two TLRs do not merge with each other or with fgTICAM-1 in resting cells. When stimulated with polyI:C, a part of the fgTLR22 population enters the cytoplasmic region to merge with fgTICAM-1 (37). Similarly upon stimulation, fgTLR3 is clustered and merges with fgTICAM-1 in the cytoplasm (37). Immunoprecipitation studies have supported their molecular interactions: fgTICAM-1 coprecipitates with fgTLR22 or fgTLR3 in human HEK293 cells. A reporter assay has shown that the dominant-negative form of fgTICAM-1 blocks the fgTLR22- and fgTLR3-mediated IFN promoter activation induced by endogenous fgTICAM-1 in RTG-2 (rainbow trout) cells. Thus, fish have a novel TICAM-1-coupling TLR, TLR22, which is clustered on the cell surface. Although mammals have lost TLR22, TLR3 is distributed on the surface membrane as well as in the endosomes only in some kinds of epithelial cells (41–44), and this appears as though TLR3 compensates for the loss of TLR22 in limited cell types.

We tested the physiological function of fgTLR22 and found that fgTLR22-expressing RTG-2 (rainbow trout) cells become resistant to virus infection (37). We used birnavirus, which is a representative dsRNA virus found in water. Cytopathic effect formation was observed in control cells that did not express fgTLR22, whereas it was barely detected in cells expressing fgTLR22. The level of TCID50 in the supernatant, which reflects virus replication in the cells, was high in the control cells and ~100-fold lower in fgTLR22-expressing cells. Virus RNA levels were suppressed in fgTLR22-expressing cells. Conversely, IFN mRNA was upregulated in virus-infected cells.

In humans, TLR3 is expressed in the endosomes and on the surface of epithelial cells/fibroblasts (18, 22). Expression of TLR3 on the cell surface membrane of human bronchial, bile-duct, and intestinal epithelial cells has also been reported

(41–44). Thus, surface-expressed human TLR3 appears to be a functional remnant of fish TLR22: TLR3 functions in the mucosal region wherein body fluids are continuously in contact with the flora. Because cell surface-associated dsRNA recognition is indispensable even in humans, TLR3 is expressed on human fibroblasts and epithelial cells. Likewise, TLR22 may be a functional substitute for human cell surface TLR3 and may act as a surveillance molecule for detecting dsRNA virus infection.

Evolution of the surface RNA recognition system in vertebrates

The results from bootstrap probability analysis indicate that TLR22 does not belong to the TLR3 family and is instead proximal to mouse TLR13, which has not been characterized as a dsRNA-recognizing TLR. Thus, two arms of the TICAM-1 pathway have evolved as dsRNA receptors in fish, and only TLR3 has been preserved in mammals (Table 1). Development of TLR22 instead of TLR3 may afford some advantage for protection against RNA viruses by augmenting the susceptibility of the local IFN response to long RNA duplexes.

We wanted to understand why teleosts require a cell surface RNA recognition system. Fish live in water and are exposed to many kinds of negative-stranded RNA viruses belonging to the Rhabdoviridae and dsRNA viruses (45, 46). Bacteria such as *Rhodovulum sulfidophilum* and perhaps other species are involved in the extracellular liberation of ribosomal and transfer RNAs into the sea (47). Thus, the sea may contain RNA viruses and RNA products of microbial origin. The sea is home to a unique and mysterious microbial environment. During evolution, vertebrates in water may have been protected from these pathogens by developing a set of RNA-sensing TLRs and an IFN system, which are distinct from those expressed in land animals. Our studies indicate that RNA sensing by TLRs protects fish from spreading or exacerbating infection. Land animals preserve the surface RNA recognition system to a limited extent in their epithelial ducts where the microbial environment is retained similar to that found in the sea.

Over-expressed teleost TLR22 protects host cells from infection with IPNV, which is a naked bisegmented dsRNA virus belonging to the family Birnaviridae (48). Birnaviruses have a single T = 13 *icosahedral* shell that is composed of 120 subunits, and these viruses lack the characteristic inner capsid. Aquatic birnaviruses are distributed worldwide, can infect a range of fish and shellfish species (45, 46), and are viral pathogens that cause diseases in fry and young fish. Although teleosts have the gene that encodes a putative ortholog of the cytoplasmic RNA sensor MDA5 (36, 49), IPNV efficiently infects teleost cells unless TLR22 is expressed in some population of cells. Thus, fish MDA5 is insufficient for protection against this type of dsRNA virus. Although all cells do not express TLR22, IFN seems to be sufficiently induced by TLR22-expressing cells to provide an antiviral environment in surrounding cells, resulting in host cell protection. However, the manner in which TLR22 detects the IPNV infection remains to be clarified. The necessity of TLR22 and its mode of dsRNA recognition in fish are of interest for further investigation.

Effector induction by endosomal TLR3 in mammals

We produced a TICAM-1 knockout (KO) mouse and tested the effector-inducing properties using the syngeneic tumor implant system of this mouse (30, 50). PolyI:C was intraperitoneally administered as the ligand for TLR3 stimulation. In this system, RLH may sense polyI:C similarly in TICAM-1 KO as well as in wildtype mice, but detectable phenotypes shouldreflect only the difference in TICAM-1 in mice. Mouse melanoma line B16

Table 1. Repertoire of pattern recognition receptors in vertebrates

	TLR															MyD88	TICAM*	RIG-I	MDA-5	IPS-1	IFN
	1	2	3*	4	5	6	7	8	9	10	12	13	14	21	22*						
Human	+	+	+	+	+	+	+	+	+	+	–	–	–	–	–	+	+	+	+	+	+
Mouse	+	+	+	+	+	+	+	+	+	*psd*	+†	+	–	–	–	+	+	+	+	+	+
Chicken	+	+	+	+	+	*psd*	+	–	–	–	–	–	+‡	+	–	+	+	–	+	*frg*	+
Xenopus	+	+	+	+	+	±	+	+	+	±	+	+	+	+	+	+	+	+	+	*frg*	+
Fugu	+	+	+	–	+	–	+	+	+	–	–	–	+	+	+	+	+	–	+	*frg*	+
Zebra	+	+	+	+	*frg*	–	*frg*	*frg*	+	–	+	–	+	*frg*	+	+	+	–	+	*frg*	+
Ascidia	~3?															–	–	–	–	–	–
Sea urchin	~300?															7	2	6?	6?	1?	–

psd, pseudogene; *frg*, fragment.
*TLR3, TLR22, and TICAM are IFN-inducing genes.
†Mouse TLR11.
‡Bird TLR15.
Ascidia and Sea urchin are invertebrate references.

[low major histocompatibility complex (MHC) expresser] and the C57BL/6 cell lines were used in this study.

The tumors grew well in wildtype mice. When polyI:C was administered intraperitoneally, tumor growth was retarded. Similar results were obtained with MyD88 KO, PKR KO, and IFN-β KO mice. PolyI:C-mediated tumor growth retardation was completely abrogated in TICAM-1 KO mice, suggesting that TICAM-1 is crucial for tumor-directed effector induction. IFN-β is an output of the activation of the TICAM-1 pathway, but it barely affects tumor regression. Retardation of tumor growth by polyI:C was completely abrogated in wildtype mice by depletion of NK1.1- or asialoGM-1-positive cells (30). Tumor growth suppression in response to polyI:C was normally observed in $CD8^+$ T-cell-depleted mice. Hence, NK/NKT cells, not CTLs, are effectors responsible for tumor regression in this mouse model with low MHC-expressing tumor. As polyI:C activates the TICAM-1 pathway, size reduction of the implant tumor reflects the potential of the effectors induced by the functioning of the TICAM-1 pathway (Fig. 5).

We next checked whether TICAM-1 in mDCs or other immune cells is important for tumor growth retardation. TICAM-1 was transfected into bone marrow-derived DCs (BMDCs), and these cells were adoptively transferred to mice with tumor burden. Tumor growth was significantly reduced in mice injected with TICAM-1-positive BMDCs but not in those injected with other BMDCs that did not express TICAM-1 (50). Thus, the mDC TICAM-1 pathway is involved in anti-tumor NK activation (30) (Fig. 5).

The TICAM-1 pathway activates transcription factors, IFN regulatory factor-3 (IRF-3), IRF-7, activator protein 1 (AP1), and NF-κB in mouse cells. The results from our *in vitro* NK assay suggest that IRF-3 largely participates in mDC-NK reciprocal activation (T. Ebihara, M. Matsumoto, T. Seya, unpublished data). Actually, polyI:C-mediated tumor growth retardation was abrogated in IRF-3 KO mice but not IRF-7 KO mice. Thus, in mDCs, induction of the molecules that drive NK activation would depend on IRF-3 activation.

We found that tumor-specific CTLs are induced by polyI:C when EG7 cells [a high MHC expresser with ovalbumin (OVA)] are employed as the implant tumor. Therefore, we checked the levels of the OVA epitope-responsive $CD8^+$ T cells, i.e. OT-1. BMDCs expressing TICAM-1 potentially induce T-cell proliferation and IFN-γ induction (Fig. 4). These T-cell responses are largely independent of IRF-3 or IRF-7 in mDCs (M. Azuma, T. Ebihara, M. Matsumoto, T. Seya, unpublished data). Thus, when implant tumor expresses high levels of MHC, CTLs driven through mDCs act as the main effector cell in mice (31). CTLs and NK cells are induced by distinct routes in mDCs (51, 52).

Cellular immune activation by mDCs depends on the situation of TLR3-adapter complex. Cytoplasmic activation of the

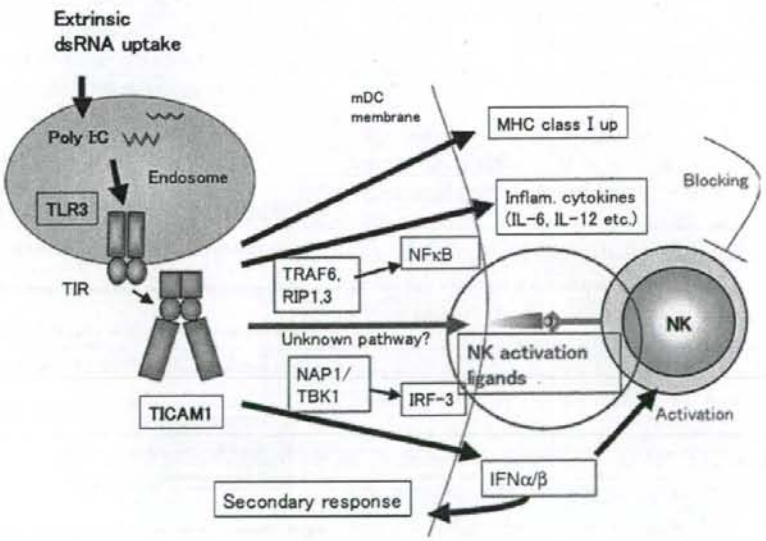

Fig. 5. Mechanism of mDC-NK reciprocal activation induced by dsRNA stimulation of mDCs. TICAM-1 has a crucial role in NK activation driven by polyI:C-stimulated mDCs in human cells. When TLR3 grasps the dsRNA signature in the endosome of mDCs, TICAM-1 in mDCs is activated to evoke a signal pathway reaching to the expression of NK-activating ligands. NK cell activation is then induced via mDC-NK contact. Some soluble factors may be important for NK activation in addition to the expression of NK-activating ligands.

mDC TICAM-1 pathway efficiently links CTL/NK activation by mDCs. Missing the cell surface-specific TLR, TLR22, and conserving ER-resident TLR, TLR3, in mDCs may cause the functional specialization of the TICAM-1 pathway on evoking cellular immunity in mammals. Although the signaling pathway by which type I IFN is induced has been elucidated in each cell type, the exact pathway that drives NK activation or CTL induction by mDCs has not been identified.

Effector induction in transgenic mice with TLR22 for surface dsRNA recognition

Upon transfection of fgTLR22 or fgTLR3 into human or mouse cells, fgTLR22 functions as an RNA sensor for IFN induction in these mammalian cells, suggesting that mice and human TICAM-1 are compatible with fish TLR22 and TLR3 (37). With this finding in mind, we have generated TLR22 transgenic (Tg) mice to test fish TLR22 antiviral function and NK activation in mouse. TLR22 is ubiquitously expressed in all the organs tested in the Tg mice (A. Matsuo, H. Oshiumi, T. Seya, unpublished data). Its expression profile is similar to that in fish, in which endogenous fish TICAM-1 is ubiquitously expressed. PolyI:C or poliovirus were used as type I IFN inducers for in vitro mouse embryonic fibroblasts (MEF) stimulation studies. TLR22-expressing MEFs produce high levels of type I IFN within 6 h, a time period during which control MEFs still do not produce type I IFN. Rapid induction and three- to fivefold higher levels of IFN-β in the supernatant are characteristic features of TLR22-expressing MEFs. Similar results were obtained with BMDCs.

The levels of NK activation induced by BMDCs do not differ significantly between TLR22-expressing BMDCs and control BMDCs. We believe that TLR22 differs from TLR3 in its ability to activate cellular immune responses. However, further investigation is necessary to establish the final conclusion.

Virus infection studies were performed on Tg mice using influenza virus and poliovirus in an in vivo mouse model (A. Matsuo, H. Oshiumi, T. Seya, unpublished data). Both Tg and control mice died of influenza infection within 7 days. It appeared that TLR22 did not protect mice from influenza. By contrast, Tg mice expressing the poliovirus receptor (PVR) and TLR22 were relatively resistant to poliovirus infection compared with TLR22-negative control PVR-Tg mice. Wildtype mice died within 5 days, but Tg mice survived for a significant longer period. Hence, TLR22 harbors antiviral activity against acute infection of dsRNA or positive-stranded RNA viruses. This TLR22 function is conserved in TLR22-positive cells of Tg mice. We support the interpretation that TLR22 is lost in mammals so that the TLR22 supplement recovers resistance to dsRNA-generating viruses. The summary of this issue on TLR22-Tg mice is illustrated in Fig. 6.

Although cell surface activation of TLR3 or TLR22 may not be associated with induction of cellular immunity, these molecules efficiently suppress acute viral infection by generating type I IFN. Development of the endosomal RNA recognition system in mDCs would be essential in mammals for enhancing the induction of cell-mediated and long-lasting immunity in viral infection. Although to what extent TLR22 participates in the induction of cellular immunity by virus infection remains largely unsettled, fish unequivocally develop the endosomal RNA recognition system involving TLR3. Cell surface RNA recognition by TLR3 exerts some toxic features (7, 53), which may facilitate limited usage of TLR3 on membrane surface. Part of the linking between TLRs and cellular immune responses should have been established before human and fish ancestors diverged.

Prototype of the vertebrate TLR system

The phylogenetic tree of vertebrate TLR family members strongly supports the notion that non-mammalian vertebrate TLRs emerged during the Cambrian period together with other mammalian TLRs (13, 14, 36, 49); thus, the human ancestor probably possessed both contemporary TLR subsets and those of non-mammalian vertebrates. Based on our knowledge of the functional coverage of vertebrate TLR family members, the expected TLR subsets that the vertebrate

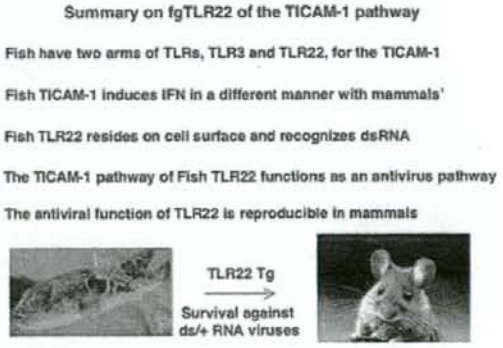

Fig. 6. Summary on fgTLR22 of the TICAM-1 pathway. (i) Fish have two arms of TLRs, TLR3, and TLR22, for the TICAM-1. (ii) Fish TICAM-1 induces IFN in a different manner with mammals. (iii) Fish TLR22 resides on cell surface and recognizes dsRNA. (iv) The TICAM-1 pathway of fish TLR22 functions as an antivirus pathway. (v) The antiviral function of TLR22 is reproducible in mammals.

common ancestor would have possessed would include at least the following 10 TLR members: TLR2, TLR3, TLR4, TLR5, TLR7, TLR8, TLR9, TLR21, TLR21, and TLR22 (13) (*Table* 1). Prior to the evolution of mammals, gene duplications would have occurred, especially in TLR2 subfamily members. Furthermore, some TLR genes were lost in some lineages, although the reason remains unknown. For example, TLR21 was diminished in the mammalian lineage, and TLR22 was lost when the mammalian ancestor began to live on land (36). Why did our human ancestor lose TLR21 and TLR22 during evolution? There are two possible explanations. First, mammals need to recognize patterns in the endosome to link the acquired responses so that non-mammalian TLRs present on the cell surface would become dispensable in the innate system. This scenario is conceivable, because the acquired system in mammals is far more sophisticated than that of teleosts. Second, the mammalian lineage happened to lose the non-mammalian TLRs. This observation is not surprising because loss of genes, which are useful for the descendant, has occurred occasionally during vertebrate evolution. For example, the vertebrate ancestor probably possessed broader spectral opsin genes for light sensing, keener auditory sensors for sound hearing, and more olfactory genes for smell sensing than humans, but the mammalian ancestor lost these outstanding genes since their divergence from reptiles (54); thus, many mammalian species are less sensitive to distal light wavelength of light, high frequency of sound, and faint smell than other non-mammalian vertebrates. If mammals had successfully reproduced TLR22 in their genomes, innate immunity in humans would have been stronger. Optional environmental pressure by pathogens may have led to the divergence of the immune system, resulting in variations. In any case, TLRs linked cellular immunity a long time ago: a common ancestor of fish and human already had a prototype. Based on this view, it appears that our immune system is not ideal but is just an example of how infections with certain pathogens have been prevented over a long time period.

References

1. Medzhitov R, Janeway CA Jr. Innate immunity: the virtues of a nonclonal system of recognition. Cell 1997;**91**:295–298.
2. Medzhitov R, Preston-Hurlburt P, Janeway CA Jr. A human homologue of the *Drosophila* Toll protein signals activation of adaptive immunity. Nature 1997;**388**:394–397.
3. Akira S, Uematsu S, Takeuchi O. Pathogen recognition and innate immunity. Cell 2006;**124**:783–801.
4. Yoneyama M, Fujita T. Function of RIG-I-like receptors in antiviral innate immunity. J Biol Chem 2007;**282**:15315–15318.
5. Matsumoto M, Seya T. TLR3: interferon induction by double-stranded RNA including poly(I:C). Adv Drug Deliv Rev 2008;**60**: 805–812.
6. Carter WA, Pitha PM, Marshall LW, Tazawa I, Tazawa S, Ts'o PO. Structural requirements of the rI n-rC n complex for induction of human interferon. J Mol Biol 1972;**70**:567–587.
7. Absher M, Stinebring WR. Toxic properties of a synthetic double-stranded RNA. Endotoxin-like properties of poly I:poly C, an interferon stimulator. Nature 1969; **223**:715–717.
8. Sasai M, Shingai M, Funami K, Yoneyama M, Fujita T, Matsumoto M, Seya T. NAK-associated protein 1 participates in both the TLR3 and the cytoplasmic pathways in type I IFN induction. J Immunol 2006;**177**: 8676–8683.
9. Honda K, Taniguchi T. IRFs: master regulators of signalling by Toll-like receptors and cytosolic pattern-recognition receptors. Nat Rev Immunol 2006;**6**:644–658.
10. Hoshino K, Kaisho T. Nucleic acid sensing Toll-like receptors in dendritic cells. Curr Opin Immunol 2008;**20**:408–413.
11. Iwasaki A, Medzhitov R. Toll-like receptor control of the adaptive immune responses. Nat Immunol 2004;**5**:987–995.
12. Reis e Sousa C. Dendritic cells in a mature age. Nat Rev Immunol 2006;**6**: 476–483.
13. Oshiumi H, Tsujita T, Shida K, Matsumoto M, Ikeo K, Seya T. Prediction of the prototype of the human Toll-like receptor gene family from the pufferfish, *Fugu rubripes*, genome. Immunogenetics 2003;**54**: 791–800.
14. Roach JC, et al. The evolution of vertebrate Toll-like receptors. Proc Natl Acad Sci USA 2005;**102**:9577–9582.
15. Baoprasertkul P, Peatman E, Somridhivej B, Liu Z. Toll-like receptor 3 and TICAM genes in catfish: species-specific expression profiles following infection with *Edwardsiella ictaluri*. Immunogenetics 2006;**58**:817–830.
16. Sullivan C, Postlethwait JH, Lage CR, Millard PJ, Kim CH. Evidence for evolving Toll-IL-1 receptor-containing adaptor molecule function in vertebrates. J Immunol 2007; **178**:4517–4527.
17. Yoneyama M, Onomoto K, Fujita T. Cytoplasmic recognition of RNA. Adv Drug Deliv Rev 2008;**60**:841–846.
18. Matsumoto M, et al. Subcellular localization of Toll-like receptor 3 in human dendritic cells. J Immunol 2003;**171**:3154–3162.
19. Ebihara T, Shingai M, Matsumoto M, Wakita T, Seya T. Hepatitis C virus-infected hepatocytes extrinsically modulate dendritic cell maturation to activate T cells and natural killer cells. Hepatology 2008;**48**: 48–58.
20. Fan S, et al. Zebrafish TRIF, a Golgi-localized protein, participates in IFN induction and NF-kappaB activation. J Immunol 2008;**180**:5373–5383.
21. Matsumoto M, Kikkawa S, Kohase M, Miyake K, Seya T. Establishment of a monoclonal antibody against human Toll-like receptor 3 that blocks double-stranded RNA-mediated signaling. Biochem Biophys Res Commun 2002;**293**:1364–1369.
22. Funami K, Matsumoto M, Oshiumi H, Akazawa T, Yamamoto A, Seya T. The cytoplasmic 'linker region' in Toll-like receptor 3 controls receptor localization and signaling. Int Immunol 2004;**16**:1143–1154.
23. de Bouteiller O, et al. Recognition of double-stranded RNA by human toll-like receptor 3 and downstream receptor signaling requires multimerization and an acidic pH. J Biol Chem 2005;**280**:38133–38145.
24. Oshiumi H, Matsumoto M, Funami K, Akazawa T, Seya T. TICAM-1, an adaptor molecule that participates in Toll-like receptor 3-mediated interferon-beta induction. Nat Immunol 2003;**4**:161–167.

25. Yamamoto M, et al. Role of adaptor TRIF in the MyD88-independent toll-like receptor signaling pathway. Science 2003;**301**: 640–643.
26. Häcker H, et al. Specificity in Toll-like receptor signalling through distinct effector functions of TRAF3 and TRAF6. Nature 2006;**439**:204–207.
27. Oganesyan G, et al. Critical role of TRAF3 in the Toll-like receptor-dependent and -independent antiviral response. Nature 2006;**439**:208–211.
28. Sharma S, tenOever BR, Grandvaux N, Zhou GP, Lin R, Hiscott J. Triggering the interferon antiviral response through an IKK-related pathway. Science 2003;**300**: 1148–1151.
29. Fitzgerald KA, et al. IKKepsilon and TBK1 are essential components of the IRF3 signaling pathway. Nat Immunol 2003;**4**:491–496.
30. Akazawa T, et al. Antitumor NK activation induced by the Toll-like receptor 3-TICAM-1 (TRIF) pathway in myeloid dendritic cells. Proc Natl Acad Sci USA 2007;**104**:252–257.
31. Schulz O, et al. Toll-like receptor 3 promotes cross-priming to virus-infected cells. Nature 2005;**433**:887–892.
32. Meylan E, Burns K, Hofmann K, Blancheteau V, Martinon F, Kelliher M, Tschopp J. RIP1 is an essential mediator of Toll-like receptor 3-induced NF-kappa B activation. Nat Immunol 2004;**5**:503–507.
33. Salem ML, Kadima AN, Cole DJ, Gillanders WE. Defining the antigen-specific T-cell response to vaccination and poly(I:C)/TLR3 signaling: evidence of enhanced primary and memory CD8 T-cell responses and antitumor immunity. J Immunother 2005;**28**: 220–228.
34. Sivori S, et al. CpG and double-stranded RNA trigger human NK cells by Toll-like receptors: induction of cytokine release and cytotoxicity against tumors and dendritic cells. Proc Natl Acad Sci USA 2004;**101**: 10116–10121.
35. Salaun B, Coste I, Rissoan MC, Lebecque SJ, Renno T. TLR3 can directly trigger apoptosis in human cancer cells. J Immunol 2006;**176**:4894–4901.
36. Oshiumi H, Matsuo A, Matsumoto M, Seya T. Pan-vertebrate Toll-like receptors during evolution. Curr Genomics 2008;**9**:488–493.
37. Matsuo A, et al. Teleost TLR22 recognizes RNA duplex to induce IFN and protect cells from birnaviruses. J Immunol 2008;**181**:3474–3485.
38. Funami K, Sasai M, Ohba Y, Oshiumi H, Seya T, Matsumoto M. Spatiotemporal mobilization of TICAM-1 in response to dsRNA. J Immunol 2007;**179**: 6827–6830.
39. Funami K, Sasai M, Oshiumi H, Seya T, Matsumoto M. Homo-oligomerization is essential for Toll/IL-1 receptor domain containing adaptor molecule-1 signaling. J Biol Chem 2008;**283**:18283–18291.
40. Bergan V, Steinsvik S, Xu H, Kileng Ø, Robertsen B. Promoters of type I interferon genes from Atlantic salmon contain two main regulatory regions. FEBS J 2006; **273**:3893–3906.
41. Rudd BD, et al. Deletion of TLR3 alters the pulmonary immune environment and mucus production during respiratory syncytial virus infection. J Immunol 2006; **176**:1937–1942.
42. Harada K, et al. Innate immune response to double-stranded RNA in biliary epithelial cells is associated with the pathogenesis of biliary atresia. Hepatology 2007;**46**: 1146–1154.
43. Cario E, Podolsky DK. Differential alteration in intestinal epithelial cell expression of toll-like receptor 3 (TLR3) and TLR4 in inflammatory bowel disease. Infect Immun 2000;**68**:7010–7017.
44. Nakamura MK, et al. Increased expression of TLR3 in human intrahepatic biliary epithelial cells at the site of ductular reaction in primary billiary cirrhosis. Hepatol Intern 2008;**2**:222–230.
45. Phelan PE, Pressley ME, Witten PE, Mellon MT, Blake S, Kim CH. Characterization of snakehead rhabdovirus infection in zebrafish (*Danio rerio*). J Virol 2005;**79**:1842–1852.
46. Nishizawa T, Kinoshita S, Yoshimizu M. An approach for genogrouping of Japanese isolates of aquabirnaviruses in a new genogroup, VII, based on the VP2/NS junction region. J Gen Virol 2005;**86**:1973–1978.
47. Ando T, Suzuki H, Nishimura S, Tanaka T, Hiraishi A, Kikuchi K. Characterization of extracellular RNAs produced by the marine photosynthetic bacterium *Rhodovulum sulfidophilum*. J Biochem 2006;**139**:805–811.
48. Coulibaly F, et al. The birnavirus crystal structure reveals structural relationships among icosahedral viruses. Cell 2005;**120**:761–772.
49. Ishii A, Kawasaki M, Matsumoto M, Tochinai S, Seya T. Phylogenetic and expression analysis of amphibian *Xenopus* Toll-like receptors. Immunogenetics 2007;**59**:281–293.
50. Akazawa T, et al. Tumor immunotherapy using bone marrow-derived dendritic cells overexpressing Toll-like receptor adaptors. FEBS Lett 2007;**581**:3334–3340.
51. Akazawa T, et al. Adjuvant-mediated tumor regression and tumor-specific cytotoxic response are impaired in MyD88-deficient mice. Cancer Res 2004;**64**:757–764.
52. Seya T, Akazawa T, Uehori J, Matsumoto M, Azuma I, Toyoshima K. Role of toll-like receptors and their adaptors in adjuvant immunotherapy for cancer. Anticancer Res 2003;**23**:4369–4376.
53. Zhou R, Wei H, Sun R, Tian Z. Recognition of double-stranded RNA by TLR3 induces severe small intestinal injury in mice. J Immunol 2007;**178**:4548–4556.
54. International Human Genome Sequencing Consortium. Finishing the euchromatic sequence of the human genome. Nature 2004;**431**:931–945.

Obstructing Shedding of the Immunostimulatory MHC Class I Chain–Related Gene B Prevents Tumor Formation

Jennifer D. Wu,[1] Catherine L. Atteridge,[1] Xuanjun Wang,[1] Tsukasa Seya,[3] and Stephen R. Plymate[1,2]

Abstract

Purpose: Clinical observations have suggested that shedding of the MHC class I chain–related molecule (MIC) may be one of the mechanisms by which tumors evade host immunosurveillance and progress. However, this hypothesis has never been proven. In this study, we tested this hypothesis using a prostate tumor model and investigated the effect of shedding of MIC on tumor development.

Experimental Design: We generated a shedding-resistant noncleavable form of MICB (MICB.A2). We overexpressed MICB.A2, the wild-type MICB, and the recombinant soluble MICB (rsMICB) in mouse prostate tumor TRAMP-C2 (TC2) cells and implanted these cells into severe combined immunodeficient mice.

Results: No tumors were developed in animals that were implanted with TC2-MICB.A2 cells, whereas all the animals that were implanted with TC2, TC2-MICB, or TC2-rsMICB cells developed tumors. When a NKG2D-specific antibody CX5 or purified rsMICB was administered to animals before tumor implantation, all animals that were implanted with TC2-MICB.A2 cells developed tumors. *In vitro* cytotoxicity assay revealed the loss of NKG2D-mediated natural killer cell function in these prechallenged animals, suggesting that persistent levels of soluble MICB in the serum can impair natural killer cell function and thus allow tumor growth.

Conclusions: These data suggest that MIC shedding may contribute significantly to tumor formation by transformed cells and that inhibition of MIC shedding to sustain the NKG2D receptor-MIC ligand recognition may have potential clinical implication in targeted cancer treatment.

Expression of murine NKG2D ligands on tumor cells has been shown to be effective in activating natural killer (NK)-mediated tumor elimination experimentally (1–4). In murine systems, identified NKG2D ligands include the retinoic acid early inducible family of proteins RAE-1 (1, 2), the minor histocompatibility antigen H60 (1, 2), and the murine ULBP-like transcript 1 (4, 5). Cells expressing these molecules are sensitive to the cytotoxicity of mouse NK cells. Ectopic expression of RAE-1 and H60 results in rejection of tumor cell lines expressing normal levels of MHC I molecule (2–4). Immunodepletion and other experiments showed that the tumor rejection is due to NK and CD8 T cells (2, 3). NKG2D neutralization *in vivo* enhances host sensitivity to carcinogen-induced spontaneous tumor initiation (6). These studies have proven the principle function of the NKG2D ligand receptor-mediated NK cell immunity in tumor rejection.

In humans, the MHC class I chain–related molecule MICA and MICB (generally termed as MIC) are the most investigated NKG2D ligands, which were proposed to play roles in tumor rejection (7–9). MIC is rarely expressed by normal human tissues but induced in most human epithelial tumors (10–13). Expression of MIC on the tumor cell surface can markedly enhance the sensitivity of tumor cells to NK cells *in vitro* and has been shown to inhibit the growth of human gliomas or small lung carcinomas in experimental models (14, 15). These studies suggested that NK cells can potentially eliminate MIC-positive tumor cells in cancer patients. However, as clinically observed, most of the human epithelial tumors are found to be MIC-positive rather than MIC-negative (10–13), which suggests the functional compromise of the MIC ligand-NKG2D receptor system in cancer patients to permit the growth of MIC-positive tumor cells. We and others have shown that tumor-derived soluble MIC as a result of tumor shedding is one of the factors causing the ineffectiveness of NKG2D-mediated immunity in cancer patients (13, 16–21). *In vitro* studies have shown that engagement of soluble MICA to NKG2D results in marked reduction in surface NKG2D expression on NK and T cells (13, 16, 21). Thus, soluble MIC is believed to induce down-modulation of NKG2D expression on systemic and tumor-infiltrated NK and T cells and thus result in functional impairment of NK and T cells in MIC-positive cancer patients (13, 16, 17). Reduction in the density of MIC expressed on the tumor cell surface due to MIC shedding from tumors is also proposed to be one of the mechanisms for tumor evasion (21).

Authors' Affiliations: [1]Department of Medicine, University of Washington; [2]Geriatric Research, Education and Clinical Center, Veterans Affairs Puget Sound Health Care System, Seattle, Washington and [3]Department of Microbiology and Immunology, Hokkaido University Graduate School of Medicine, Sapporo, Japan

Received 5/19/08; revised 8/12/08; accepted 8/20/08.

Grant support: DOD-USMRC New Investigators Grant W81XWH-04-1-0577 and IDEA Development Award W81XWH-06-1-0014, NW Prostate SPORE Program, and NIH Temin Award 1K01CA116002 (J.D.Wu).

The costs of publication of this article were defrayed in part by the payment of page charges. This article must therefore be hereby marked *advertisement* in accordance with 18 U.S.C. Section 1734 solely to indicate this fact.

Requests for reprints: Jennifer D. Wu, Department of Medicine, University of Washington, 325 9th Avenue, Box 359625, Seattle, WA 98104. Phone: 206-341-5349; Fax: 206-341-5302; E-mail: wuj@u.washington.edu.

doi:10.1158/1078-0432.CCR-08-1305

Translational Relevance

In humans, the MHC class I chain-related molecules MICA and MICB (generally termed MIC) are frequently found expressed on epithelial-originated tumor cells. MIC is a ligand for the activating NK cell receptor NKG2D. Engagement of tumor-expressed MIC to NKG2D can activate NK cell tumor-lytic activity *in vitro*. Thus, expression of MIC on tumor cells is proposed to play a significant role in tumor immunosurveillance. However, as observed in many cancer patients, majority of the tumors remain MIC positive, suggesting the ineptness of the NKG2D-mediated NK cell function. We and others have shown that shedding of MIC by tumor cells can impair NK cell function in cancer patients. These clinical studies prompted the hypothesis that tumor shedding of MIC may be one of the mechanisms by which MIC-positive tumors evade NK cell immunosurveillance and progress. This study tested this hypothesis *in vivo* using a prostate tumor model and for the first time showed that interfering with shedding of MIC could prevent tumor formation. Our study suggests that shedding of MIC may contribute significantly to tumor formation by transformed cells and thus inhibiting tumor shedding of MIC may have potential therapeutic implication in targeted cancer therapy.

These compelling clinical data suggest that MIC shedding from tumor cells is likely associated with tumor progression, which has prompted the hypothesis that tumor shedding of MIC is the mechanism by which MIC-positive tumors evade NK cell immunosurveillance and progress in cancer patients. However, it is impossible to test this hypothesis clinically. Taking the advantage that human MICB can be recognized by mouse NKG2D (22, 23) and that only the extracellular $\alpha1\alpha2$ domain of MIC interacts with NKG2D (24–26), here we test the hypothesis experimentally that shedding of MIC permits tumor growth and that sustained interaction between NKG2D and membrane-integrated form of MIC can cause tumor rejection. Using a well-characterized prostate tumor model TRAMP-C2 (TC2; ref. 27), we show for the first time that expression of the shedding-resistant but not the natural form of MICB prevents tumor formation by transformed cells.

Materials and Methods

Cells. TC2 cell line (gift of Dr. N.M. Greenberg, Fred Hutchinson Cancer Research Center) was maintained in DMEM as described (27). RMA-Rae-1β cells (gift of Dr. D. Raulet, Berkeley) was maintained in RPMI 1640 supplemented with 10% FCS. Eco-phoenix cells (Orbigen) were maintained in DMEM supplemented with 10% fetal bovine serum.

DNA construction, transfection, and transduction. cDNA encoding full-length human MICB (allele 0101; ref. 28) was kindly provided by Dr. A. Steinle (University of Tubingen) and subcloned into the retroviral vector pBMNZ-IRES-GFP (Orbigen). To generate recombinant soluble MICB (rsMICB), cDNA encoding the extracellular domain of MICB was amplified by PCR. To generate a putative shedding-resistant form of MICB (designated as MICB.A2), amino acids 215 to 274 of MICB were replaced with the comparable sequence of the α3 domain of HLA-A2 using recombinant PCR of the cDNA sequences (29). rsMICB-FLAG fusion peptide was generated by tagging the cDNA sequence of FLAG (DKYDDDK) to the 3′-end of the rsMICB cDNA using PCR. Error-free amplified cDNAs were identified by sequencing and subcloned into the retroviral vector pBMNZ-IRES-GFP (Orbigen). Plasmids were transfected into Eco-phoenix packaging cells to generate retrovirus. TC2 cells were transduced with respective retrovirus. Stable GFP-positive cell population was isolated by drug selection and sorted by flow cytometry.

Affinity purification of rsMICB and rsMICB-FLAG peptides. The HiTrip NHS-activated column (GE Healthcare) was conjugated with the monoclonal antibody (mAb) 6D4.6 (Santa Cruz Biotechnology) before loading with conditioned medium from TC2-rsMICB or TC2-rsMICB-FLAG cells. After washing, rsMICB or rsMICB-FLAG was eluted with 100 mmol/L sodium citrate (pH 2.5) and neutralized immediately with 1.5 mol/L Tris (pH 8.8).

Immunoprecipitation and Western blotting. Supernatant was collected from TC2-MICB cell culture and passed through a 0.45 μm filter to remove cell debris. Cells were washed and lysed with lysis buffer [50 mmol/L HEPES (pH 7.5), 150 mmol/L NaCl, 1.5 mmol/L $MgCl_2$, 1 mmol/L EGTA, 1% Triton X-100]. Clear supernatant and lysates were incubated with the mAb 6D4.6. Immunocomplexes were collected using protein A/G-agarose (Pierce). PNGase F (New England Biolabs) treatment was carried overnight at 37°C. Immunocomplexes were separated on a 4% to 15% SDS-PAGE, blotted onto a nitrocellulose membrane, and probed with goat anti-MICB antibody AF1599 (R&D Systems). Immunoreactive proteins were detected by incubating the blot with a horseradish peroxidase-conjugated secondary antibody (Pharmacia) and enhanced chemiluminescence reagents (Pharmacia).

MICB shedding assay and (s)MICB ELISA. Cells were seeded at the density of 4×10^5 per well in a 6-well plate in complete medium overnight and replaced with 1 mL/well serum-free medium for 6 h. Supernatant was collected and filtered through 0.45 μm filter. Cells were lysed with 1 mL lysis buffer. Amount of soluble MICB in the supernatant and MICB in the cell lysates was measured using human MICB DuoSet sandwich ELISA kit (R&D Systems). For measuring mouse serum levels of soluble MICB, serum was diluted 1:2 with PBS for ELISA assay.

In vivo study. Animal studies were approved by the Institutional Animal Care and Use Committee. Six to 10 severe combined immunodeficient (SCID) male mice (6-week old Harlan-Sprague-Dawley) were used in each group. The following cells (1×10^6 per mouse) were subcutaneously injected into respective group of animals: TC2, TC2-MICB, TC2-MICB.A2, and TC2-rsMICB. All animals were monitored for tumor growth for up to 12 weeks. Tumor volume was estimated using the formula: $V = L \times W^2 / 2$. Animals were euthanized when tumor volumes reached 1,000 mm^3. Tumors, spleens, and peripheral blood were terminally collected. Serum was separated by centrifugation and used for rsMICB ELISA.

In vivo NKG2D blocking or neutralization. To block NKG2D receptor, 100 μg of the functional grade of anti-NKG2D blocking antibody CX5 (eBiosciences) were injected intraperitoneally on the day before and the day after tumor implantation and thereafter every 3 days. Blocking was confirmed by flow cytometry of peripheral lymphocytes collected from orbital sinus bleeding with PE-conjugated CX5 (eBiosciences). To modify NKG2D function, animals were injected intraperitoneally with 50 ng purified rsMICB before implantation of TC2-MICB.A2 cells and thereafter twice a week for 4 weeks. Blood was collected once a week from sinus orbital bleeding and serum levels of rsMICB were measured by ELISA.

Flow cytometry. For detection of cell surface expression of NKG2D ligands, TC2 and its derivative cells were trypsinized, blocked with anti-mouse CD16/CD32 (eBiosciences), and incubated with anti-MICA/B mAb 6D4.6 or anti-MICB MAB1599 (R&D Systems) or anti-pan-RAE-1 mAb17582 (R&D Systems) followed by a PE-conjugated secondary

reagent. For detection of rsMICB expression, the BD Cytofix/Cytoperm kit (BD Sciences) was used. Briefly, TC2-rsMICB cells were cultured in the presence of BD GolgiPlug for 3 h to prevent the secretion of rsMICB before harvesting. Cells were resuspended in BD fixation/permeabilization solution for 20 min at 4°C and incubated with 6D4.6 followed with PE-conjugated secondary reagents. For mouse NKG2D binding assay, cells were incubated with 10 μg/mL of the fusion protein of recombinant soluble mouse NKG2D and human Fc (smNKG2D-Fc; R&D Systems) followed by PE-conjugated $F(ab')_2$ goat anti-human IgG. For H-$2K^b$ expression, cells were incubated with $Alex^{647}$-conjugated anti-H-$2K^b/D^b$ mAb (Biolegend).

Single-cell suspensions of splenocytes were prepared as described (30). Cells were stained with FITC-conjugated mAb DX5 (eBiosciences) and PE-conjugated anti-mouse NKG2D mAb CX5 (eBiosciences) or A10 (eBiosciences) and analyzed using a BD FACScan or LSRII. For *ex vivo* rsMICB competitive binding assay, freshly isolated splenocytes were incubated with 10 ng/μL rsMICB-FLAG followed with FITC-conjugated mAb M2 (Sigma-Aldrich) and PE-conjugated mAb DX5 (eBiosciences). Data were analyzed using the BD CellQuest^{Pro} (BD Biosciences) or FlowJo software (Tree Star).

Cytotoxicity assay. Fresh NK cells were prepared using $Spin^{sep}$ murine NK enrichment cocktail (Stem Cell Technology) and were >90% $DX5^+$. LAK cells were prepared by culturing NK cells for 4 to 7 days in 1,000 units/mL recombinant human interleukin-2. Cytotoxicity was done in triplicates using the standard 4 h ^{51}Cr release assay (13). Antibody blocking was done by preincubating effector cells with 30 μg/mL NKG2D blocking mAb CX5 (eBiosciences) or preincubating target cells with 100 μg/mL anti-pan RAE-1 polyclonal antibody at 37°C for 1 h (31).

Statistical analysis. Data were analyzed using JMP software. Significance between two animal groups was determined by Student's *t* test. $P < 0.05$ was considered significant.

Results

Putative cleavage region of MIC(B) in TC2 tumor cells. TC2 is a mouse prostate tumor cell line generated from the TRAMP mouse (27), which does not express any homologous molecules to human MIC (28). TC2 cells were transduced with retroviruses that carry cDNAs of human MICB and GFP. Transduced cells stably expressing high levels of MICB (designated as TC2-MICB cells) were generated by puromycin selection and multiple rounds of flow cytometry cell sorting for GFP-positive cells.

To generate a shedding-resistant form of MICB, we first performed experiments to predict putative cleavage region of MICB by tumor cells. Soluble MICB resulted from TC2 shedding (designated as ssMICB) was immunoprecipitated from supernatant of TC2-MICB cells with a mouse mAb 6D4.6 specific to the α1α2 ectodomain of MICA/B (10). The full-length MICB was immunoprecipitated from cell lysates with the same antibody. Immunocomplexes were separated and immunoblotted with a goat polyclonal antibody AF1599 specific to the ectodomain of MICB. After N-glycosidase (PNGase F) treatment, ssMICB yield two bands of molecular mass ~31 to 33 kDa (Fig. 1A). The molecular mass is consistent with other studies showing soluble MICB and soluble MICA released by human tumor cells (32, 33). When samples were treated with dinitrothiocyanobenzene, a disulfide isomerase inhibitor, only a single band of soluble MICB was revealed (data not shown), suggesting that the two bands of soluble MICB released by TC2 cells are the reduced and nonreduced forms of ssMICB. Similar observation of soluble MICA shed by human tumor cell lines was shown by Kaiser et al. (33). The deglycosylated full-length MICB is shown to be ~41 kDa in the cell lysates (Fig. 1A), consistent with other studies (34). Although the precise cleavage site cannot be determined, these data suggest that MICB was cleaved at the α3 domain proximal to the transmembrane region to generate ssMICB (Fig. 1B). Similar cleavage region is also predicted for human tumor cell lines to generate soluble MICA (33).

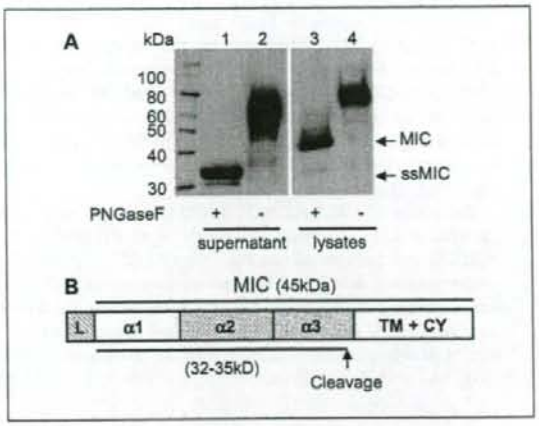

Fig. 1. Putative MICB cleaved site(s) in TC2 cells. *A*, Western blot showing the predicted size of cleaved soluble MICB in TC2 cells. Supernatant and lysates of TC2-MICB cells were immunoprecipitated with anti-MIC mAb 6D4.6. The immunocomplexes were treated with PNGase F and resolved on SDS-PAGE. Proteins were transferred to nitrocellulose membrane and blotted with goat anti-MICB polyclonal antibody. *Lanes 1* and *2*, detection of soluble MICB from TC2-MICB supernatant. The molecular mass of the deglycosylated cleaved soluble MICB is estimated to be 31 to 33 kDa. *Lanes 3* and *4*, detection of full-length MICB from TC2-MICB cell lysates. The full-length deglycosylated MICB is estimated to be 41 kDa on 4% to 15% SDS-PAGE. *B*, putative MICB cleavage site(s).

Generation of tumor cell lines expressing the putative shedding-resistant MICB.A2 and rsMICB. To study the effect of MIC shedding on tumor formation and growth *in vivo*, we generated two forms of MICB, the recombinant secretable form of MICB (rsMICB) and a putative shedding-resistant form of MICB (MICB.A2). rsMICB was generated by deletion of the transmembrane and cytoplasmic domains. MICB.A2 was generated by replacing part of the α3 domain of MICB (amino acids 215-274) with the corresponding residues from HLA-A2 (Fig. 2A). Because NKG2D only interacts with the α1α2 domain of MIC (24), MICB.A2 would presumably continue to recognize NKG2D. rsMICB and MICB.A2 were overexpressed in TC2 cells using the GFP retroviral system described above. Positive-expressing clones were selected by puromycin and repeated sorting by flow cytometry for GFP-positive cells. The expression level of cellular rsMICB and surface MICB.A2 in TC2 cells was confirmed by flow cytometry with the anti-MIC mAb 6D4.6 (Fig. 2B).

Partial replacing the α3 domain of MICB protects from tumor cell shedding. An ELISA assay was used to assess the degree of shedding of MICB and MICB.A2 in TC2 cell lines. Both the capture and the detection antibodies are specific to the extracellular domain of MICB and can also detect MICB.A2 by Western blotting (data not shown). With a given number of cells, the amount of cleaved soluble MIC in the culture supernatant and the amount of MIC in the lysates were

measured by a sandwich ELISA assay (Fig. 2C). The degree of MIC shedding was estimated by the molar percentage of soluble MICB released into the supernatant. Approximately 30% of MICB was cleaved into the medium in TC2 cells, whereas no cleaved form of MICB.A2 was detectable in the culture supernatant (Fig. 2C). This indicates that MICB.A2 cannot be cleaved into soluble forms by tumor cells and is shedding-resistant.

Expression of MICB.A2 in TC2 cells stimulates mouse NK cell cytolytic activity. Human MICB can be recognized by mouse NKG2D and activate mouse NK cells (22, 23). To test whether overexpressing MICB.A2 can also activate mouse NK cells, we first addressed the physical interaction of MICB.A2 with soluble mouse NKG2D-Fc (smNKG2D-Fc) fusion protein by flow cytometry analyses. As measured by mean fluorescence intensity (Fig. 3A), smNKG2D-Fc was more prominently bound by TC2-MICB and TC2-MICB.A2 cells and only weakly bound by TC2 and TC2-rsMICB cells. Accordingly, *in vitro* cytotoxicity assay revealed marked increase in sensitivity of TC2 cells to interleukin-2-activated mouse NK (LAK) cells when MICB or MICB.A2 was overexpressed (Fig. 3B; $P < 0.01$). The increased susceptibility of TC2-MICB and TC2-MICB.A2 cells to LAK cells can be inhibited by preincubation of LAK cells with the NKG2D-specific blocking antibody CX5 (ref. 35; Fig. 3B), suggesting a NKG2D-dependent LAK cell-killing effect. Thus, the shedding-resistant MICB.A2 maintained the functional property of MICB to be recognized by mouse NKG2D.

Although not expressing any MIC homologue, TC2 cells express some levels of endogenous NKG2D ligand RAE-1 variants but not H60 (22, 36). However, the level of endogenous NKG2D ligands is not sufficient to stimulate LAK cell *in vitro* cytotoxicity (Fig. 3B). To address whether the increased

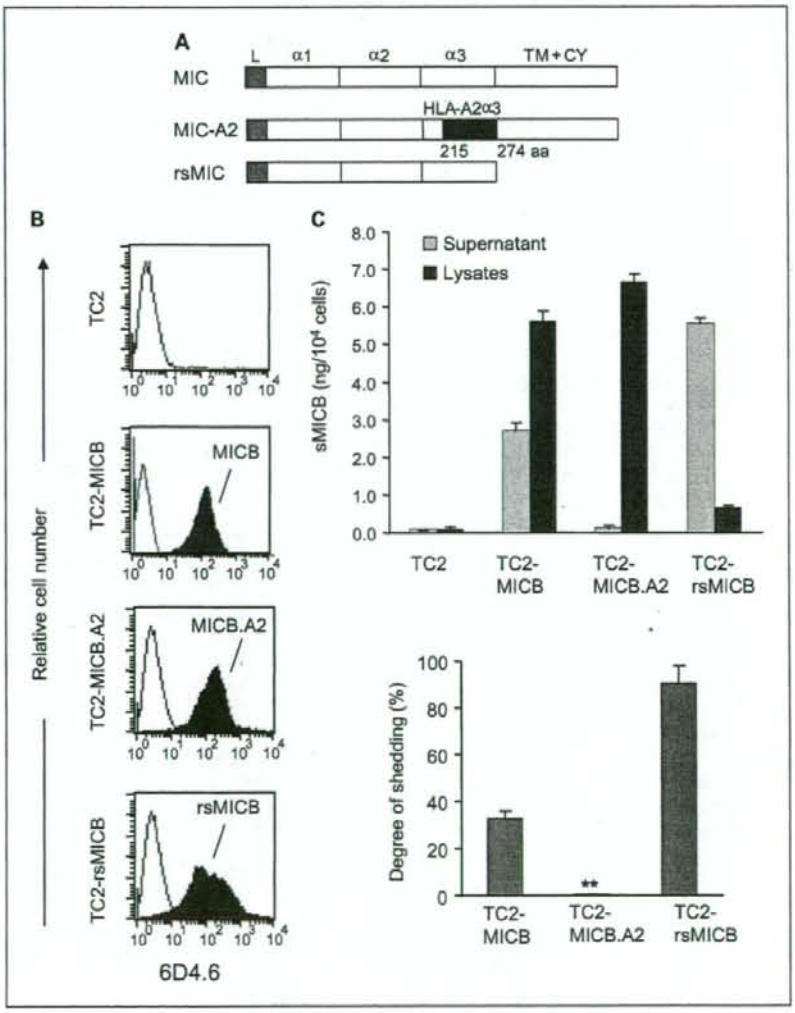

Fig. 2. Construction and expression of the shedding-resistant noncleavable and soluble recombinant forms of MICB (rsMICB) in TC2 cell lines. *A*, generation of the noncleavable form MICB.A2 by replacing amino acids 215 to 274 of the MICB α3 domain with the corresponding sequence of HLA-A2. rsMICB was generated by deletion of the entire transmembrane and cytoplasmic region of MICB. *B*, flow cytometry showing expression levels of MICB, MICB.A2, and rsMICB in TC2 cell lines. cDNAs of MICB, MICB.A2, or rsMICB were inserted into a IRES-GFP retroviral vector pBMNZ. TC2 cells were transduced with respective retrovirus. GFP-positive cells were sorted by flow cytometry. For detection of MICB and MICB.A2 expression, cells were directly incubated with anti-MIC 6D4.6 antibody followed a PE-conjugated secondary reagent. For detection of the secretable rsMICB expression, TC2-rsMICB cells were cultured in the presence of BD GolgiPlug for 3 h to prevent the secretion of rsMICB before harvesting. Cells were resuspended in BD Fixation/Permeabilization solution for 20 min at 4°C and incubated with 6D4.6 followed with a PE-conjugated secondary reagent. *C*, MICB.A2 is shedding-resistant. *Top*, amount of shed soluble MICB in the culture supernatant and MICB in the cell lysates. Cells (4×10^5 per well) were plated on a 6-well plate overnight. Medium was removed and replaced with 1 mL serum-free medium. Six hours later, medium was collected and filtered. Cells were lysed with 1 mL lysis buffer, and 50 μL culture supernatant and cell lysates were used for (s) MICB ELISA assay. *Bars*, SE. *Bottom*, degree of shedding as calculated by molars of soluble MICB in the supernatant versus total molars of soluble MICB and MICB (a sum of supernatant and cell lysates). Final results were normalized by cell numbers at the time of the assay. Results of three independent experiments. *, $P < 0.001$.

sensitivity of TC2-MICB and TC2-MICB.A2 cells to LAK cell killing is possibly due to increased expression of RAE-1, we analyzed endogenous RAE-1 expression on these cell lines by flow cytometry with a rat anti-pan RAE-1 mAb. A consistency of RAE-1 expression among TC2, TC2-MICB, and TC2-MICB.A2 cell lines is shown in Fig. 3C. Furthermore, preincubation of target cells with an anti-pan RAE-1 blocking antibody (30) did not significantly reduce the susceptibility of TC2-MICB or TC2-MICB.A2 cells to LAK cells, whereas the sensitivity of the control RMA-Rae-1β cells to LAK cells was significantly reduced (Fig. 3B). These suggest that the increased killing of TC2-MICB or TC2-MICB.A2 cells by LAK cells is not due to increased RAE-1 expression.

TC2 cells express a very low level of H-2K^b/D^b (37), which is a potential ligand for inhibitory Ly49 receptor families. We analyzed H-2K^b/D^b expression on these cell lines by flow cytometry. Consistent levels of H-2K^b/D^b expression were found in TC2 and cell lines expressing MICB or MICB.A2 (Fig. 3C), suggesting that the increased sensitivity of TC2-MICB and TC2-MICB.A2 cells to LAK cells was not attributed to a reduced level of H-2K^b/D^b expression.

Shedding-resistant MICB.A2 but not the natural MICB prevents TC2 tumor formation **in vivo.** In three independent experiments, when SCID animals were implanted with TC2-rsMICB, TC2-MICB, or TC2-MICB.A2 cells, none of animals that were implanted with the TC2-MICB.A2 cells developed tumors with a 12-week follow-up observation period, whereas all the animals that were implanted with TC2-rsMICB or TC2-MICB cells developed tumors within 3 weeks (Fig. 4A and B). In addition, no significant difference in tumor growth was observed among TC2, TC2-rsMICB, and TC2-MICB originated tumors (Fig. 4A). To address whether the failure to reject TC2-MICB tumors is due to the large dose (1×10^6) of tumor cells injected, we repeated the experiment with TC2-MICB and TC2-MICB.A2 cells using smaller numbers of inoculated cells. A 10-fold (1×10^5) and a 100-fold (1×10^4) decrease in the number of inoculated tumor cells did not change the outcome (Fig. 4C). We also examined MICB expression in the TC2-MICB-originated tumor cells extracted from SCID animals by flow cytometry. All the extracted tumor cells expressed the similar levels of MICB before implantation (Fig. 4D). This suggests that tumor growth in animals that were implanted with TC2-MICB cells is not due to NK cells selectively eliminating MICB-positive cells.

Shedding of MICB by TC2 cells allows TC2-MICB tumor growth in mice. In 4 h *in vitro* cytotoxicity assays, both TC2-MICB and TC2-MICB.A2 cells were sensitive to LAK cells (Fig. 3B). However, NK tumor immunity was effective only in animals when the noncleavable MICB.A2 was expressed on tumor cells. We propose that the discrepancy of *in vivo* and *in vitro* observation is attributed to tumor cell shedding of MICB *in vivo*, which accumulatively compromises NK cell function in animals implanted with MICB-expressing tumor cells. To test this hypothesis, we measured serum levels of soluble MICB in all the animals 4 weeks after tumor implantation using a sandwich ELISA assay. A significant level of soluble MICB was detected in the sera of animals that were implanted with tumor cells expressing rsMICB and MICB, whereas no soluble MICB was detectable in animals implanted with tumor cells expressing MICB.A2 (Fig. 5A). To address why TC2-MICB cells were sensitive to LAK cell *in vitro*, LAK cells were incubated with the supernatant of TC2-MICB cells for various periods and used as

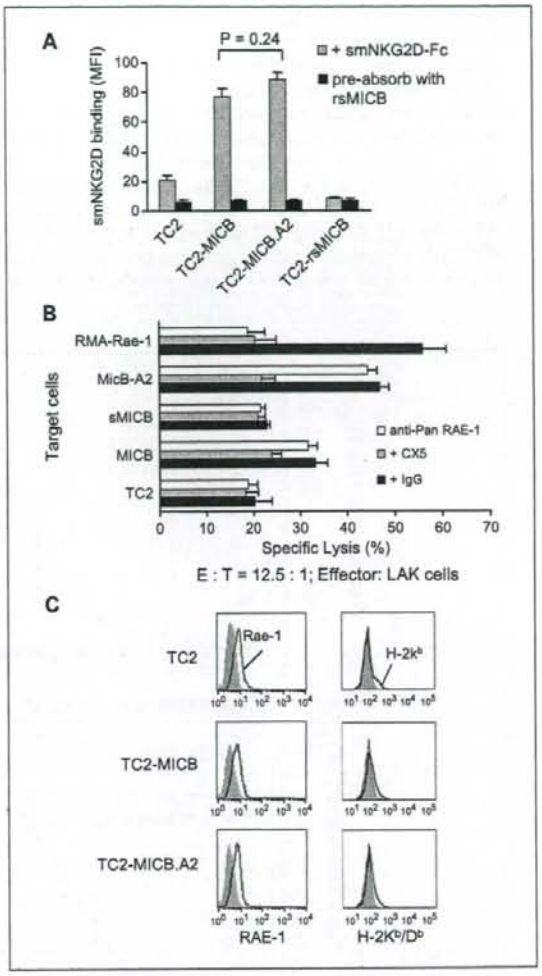

Fig. 3. Overexpression of MICB and MICB.A2 increases the sensitivity of TC2 cells to NK cell killing. *A*, binding of MICB and MICB.A2 by mouse NKG2D. Cells were incubated with the chimeric soluble mouse NKG2D-human Fc (smNKG2D-Fc) followed by PE-conjugated anti-human IgG. Cells were analyzed by flow cytometry. Data are mean fluorescence intensity. When smNKG2D-Fc was preabsorbed with rsMICB, no binding was seen in any of the cell lines. No significant difference was shown in the binding ability between MICB and MICB.A2 ($P = 0.24$). *B*, sensitivity of various MICB-expressing TC2 cells to mouse NK cells. NK cells were isolated from SCID mice and cultured in complete medium with 1,000 units/mL interleukin-2 for 4 d before used as effectors in standard 4 h ^{51}Cr release assay. For blocking NKG2D receptor, effector cells were preincubated with 30 μg/mL CX5 antibody. For blocking RAE-1, target cells were preincubated with 100 μg/mL anti-pan-RAE-1 polyclonal antibody for 1 h before the assay. RMA-Rae-1β cells were used as positive controls for blocking antibodies. *E:T*, effector:target ratio. *Bars*, SE. *, $P < 0.01$, compared with TC2 cells as targets. *C*, flow cytometry histograms showing surface expression of RAE-1 (*left*) and H-2K^b/D^b (*right*) in TC2, TC2-MICB, and TC2-MICB.A2 cells. *Filled histograms*, cells were stained with control isotype antibodies; *open histograms*, cells were stained with specific antibodies. Results of three independent experiments.

effector cells to kill target TC2-MICB.A2 cells. Only after 8 h incubation, LAK cell-killing ability was significantly affected. Therefore, in the 4 h *in vitro* cytotoxicity assay, the killing ability of LAK cells was not significantly affected by soluble MICB

resulted from target TC2-MICB cells (data not shown). We further examined NK cell tumor-killing ability from these animals. For this purpose, freshly isolated splenic NK cells were used as effector cells for *in vitro* cytotoxicity assay. NK cells from mice bearing MICB- and rsMICB-expressing tumors had a significant reduction in cytotoxicity against TC2-MICB.A2 target cells in comparison with those from TC2 tumor-bearing or tumor-free animals ($P < 0.01$; Fig. 5B). The cytotoxicity of these NK cells was inhibited by preincubating with a NKG2D-specific inhibitory mAb CX5 (Fig. 5B), suggesting a NKG2D-dependent effect. Together, these results suggest that persistent presence of soluble MICB *in vivo* due to tumor cell shedding of MICB compromised NKG2D-mediated NK cell lytic activity and thus permitted the growth of MICB-expressing tumor cells.

Persistent presence of soluble MICB blocks the NKG2D-mediated NK cell recognition of target cells. When animals were treated with the CX5 antibody to block NKG2D receptor, injection of TC2-MICB.A2 cells gave rise to tumor formation in all the SCID animals (Fig. 6A). This suggests that the inhibition of TC2-MICB.A2 tumor formation in SCID animals is NKG2D-dependent. To test the effect of presence of soluble MICB on tumor formation of MICB.A2-expressing cells, we injected animals with purified rsMICB (50 ng) before and after implanting TC2-MICB.A2 cells. Under this experimental

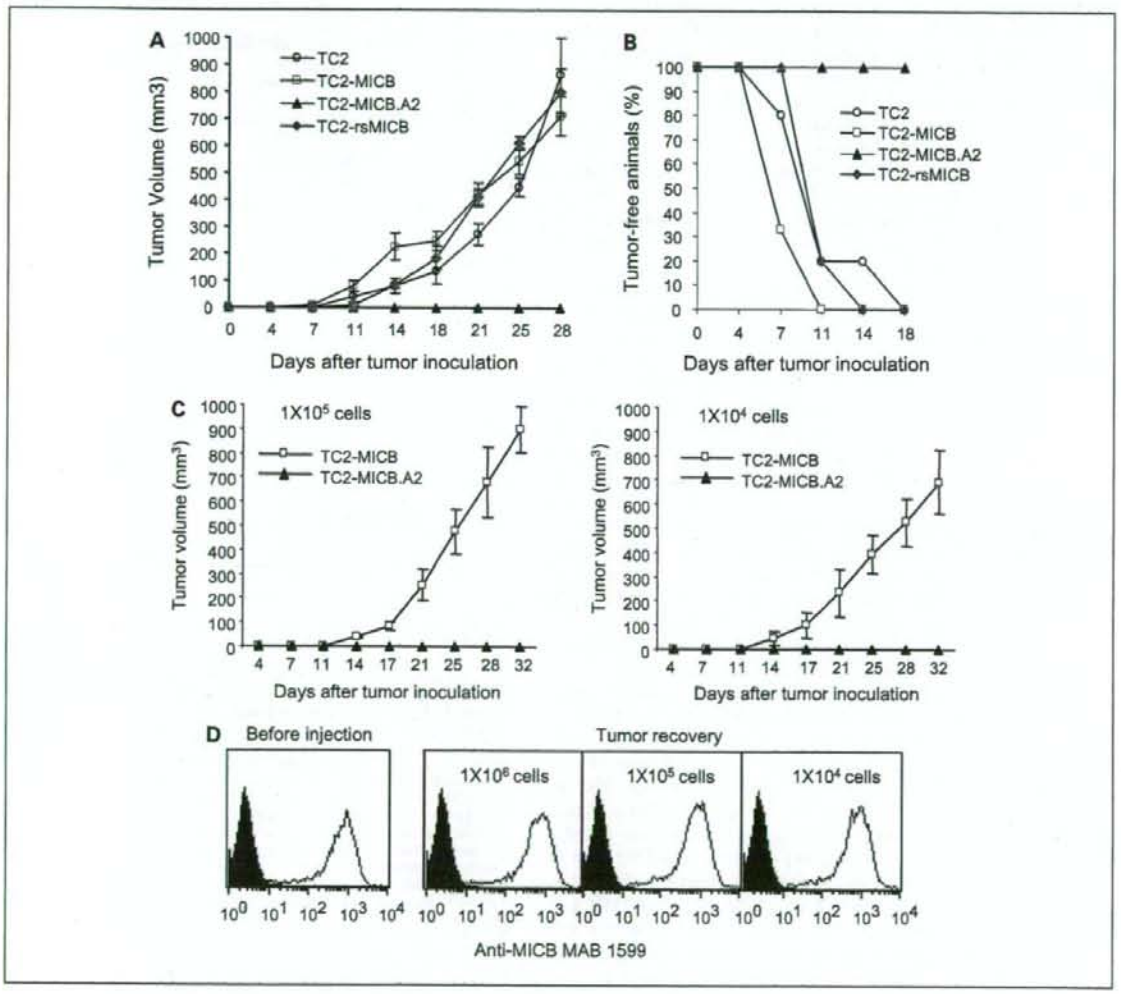

Fig. 4. Expression of MICB.A2 but not the cleavable MICB prevents tumor formation *in vivo*. Six animals were used in each group. Tumor growth was monitored twice weekly. Tumor volume was estimated by the formula: $V = L^2 \times W / 2$. *A*, tumor growth of various MICB-expressing TC2 cells in SCID mice. *B*, rate of tumor formation of various MICB-expressing TC2 cells in SCID mice. Cells (1×10^6) were injected subcutaneously into each animal in *A* and *B*. *C*, tumor growth of TC2-MICB cells when injected at lower doses (1×10^5 and 1×10^4 cells per animal). *D*, representative flow cytometry histoplots showing MICB expression in tumor cells extracted from animals inoculated with TC2-MICB cells compared with prior inoculation. The MICB-specific antibody MAB1599 (R&D Systems) was used as primary antibody. *Filled histogram*, MICB expression in TC2 cells; *open histogram*, MICB expression in TC2-MICB cells or tumor cells. Results of three independent experiments.

condition, implantation of TC2-MICB.A2 cells gave 100% tumor formation (Fig. 6A). Tumor cells extracted from these animals were shown to be GFP-positive and express MICB.A2 by flow cytometry analyses (data not shown). NK cells isolated from these animals showed very little cytolytic activity against TC2-MICB.A2 target cells (data not shown). These data suggest that persistent presence of soluble MICB compromises the cytotoxicity of NK cells against TC2-MICB.A2 cells.

We sought the mechanisms by which tumor shedding-derived soluble MICB would diminish NK cell activity. Soluble MICB may down-modulate surface NKG2D expression on NK cells (16) or block the recognition of NK cells to target cells by physical occupancy of the NKG2D receptor. To distinguish these two mechanisms, we first analyzed NKG2D expression on splenic NK cells freshly isolated from animals injected with various TC2 tumor cells using flow cytometry analyses with a nonblocking NKG2D antibody A10 (29). There was no significant difference in surface NKG2D expression on NK cells from mice bearing TC2-MICB and TC2-rsMICB tumors compared with those from animals bearing TC2 tumors or tumor-free animals (Fig. 6B), suggesting that the suppressive effect of soluble MICB on NK cell activity was not through down-modulation of surface NKG2D receptor. We further examined the occupancy of NKG2D receptor on NK cells by tumor-derived soluble MICB using competitive binding assay. Freshly isolated splenocytes were incubated with purified rsMICB-FLAG, and NK cell-binding ability to rsMICB-FLAG was measured by flow cytometry using the anti-FLAG mAb M2.

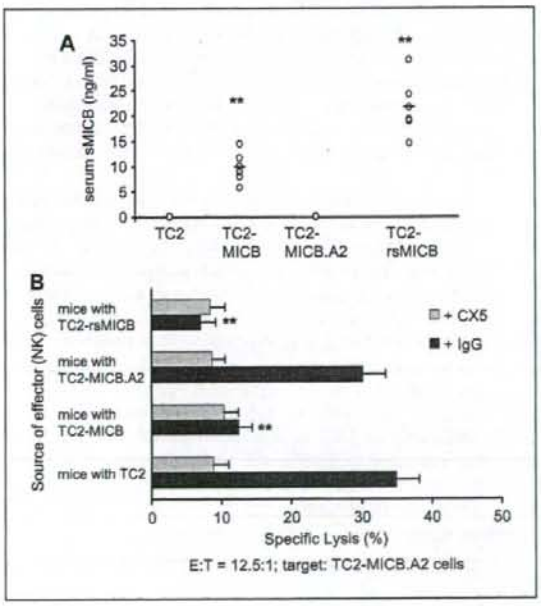

Fig. 6. Shedding of MICB by TC2-MICB cells compromises NK cell activity *in vivo*. *A*, serum levels of soluble MICB in all the tumor-bearing animals. *B*, reduced NKG2D-dependent NK cell cytotoxicity of splenic NK cells from animals bearing TC2-rsMICB and TC2-MICB tumors. Freshly isolated NK cells were used as effectors; TC2-MICB.A2 cells were used as target cells. **, $P < 0.01$, compared with TC2 or TC2-MICB.A2. Results of three independent experiments.

NK cells from animals inoculated with TC2-MICB or TC2-rsMICB cells had significantly reduced binding to rsMICB-FLAG compared with those from animals inoculated with TC2 or TC2-MICB.A2 cells ($P < 0.01$; Fig. 6C). Together, these data suggest that soluble MICB dampens NKG2D-dependent NK cell activity mainly by masking the NKG2D receptor and thus blocking the interaction of NKG2D with target molecules.

Discussion

This study has provided conclusive evidence supporting the hypothesis that shedding of MIC by transformed cells can promote tumor growth. In this study, we generated a shedding-resistant NKG2D ligand MICB.A2 by partially modifying the α3 domain of MICB and showed that overexpressing MICB.A2 prevented tumor formation by the mouse prostate tumor cell line TC2. We also showed that, when soluble MICB was persistently present, expression of the shedding-resistant MICB.A2 on the tumor cell surface did not prevent or delay tumor formation *in vivo*. Our study signifies the effect of MIC shedding on tumor formation and the magnitude of sustained MIC-induced NKG2D immunity in preventing early tumor development.

Although the mechanisms of MIC shedding is still under investigation (19, 33, 38), clinical evidence has shown that shedding of MIC is common in MIC-positive cancers, such as prostate, colon, breast adenocarcinomas, and melanomas (10–13). In these patients, the function of NK and/or CD8 T cells was compromised due to soluble MIC-induced internalization of the NKG2D receptor (13, 16–18). Thus, it was hypothesized that MIC shedding in tumors can promote tumor immune evasion and progress to advanced disease. Recent studies have shown that MIC expression is not restricted in tumor cells and that MIC can be induced in cells in response to DNA damage (39), a prior event to transformation. Therefore, the current study indicates that, in the event of malignant transformation, inhibiting shedding of MIC from MIC-positive transformed cells can prevent the initiation of tumor formation.

We chose to overexpress human MICB rather than mouse NKG2D ligands in this study for the following rationales. Firstly, MIC has been shown to be shed by tumor cells in cancer patients; thus, the study is clinically relevant. Secondly, MICB has been shown to interact with mouse NKG2D, and MICB-positive cells are sensitive to mouse NK cells (22, 23). We also have shown that MICB was shed by the mouse prostate cell line TC2 in the same pattern as MIC shedding in prostate cancer patients.[4] Thirdly, although mouse NKG2D ligands are functionally similar to human MIC in NK cell activation, these molecules are structurally different and may have different physiologic roles. Mouse NKG2D ligands lack the α3 domain and are mostly GPI-linked proteins (9); in addition, little is known about what controls the expression of mouse NKG2D ligands *in vivo* and whether they would shed in a similar fashion to MIC in human tumor cells. Lastly, different from human NKG2D ligands, studies have shown that naturally expressed mouse NKG2D ligands on tumor cells may not cause tumor rejection largely due to insufficient levels of the ligand expression (2) or low affinity of binding to NKG2D (40). In

[4] Wu, unpublished data.

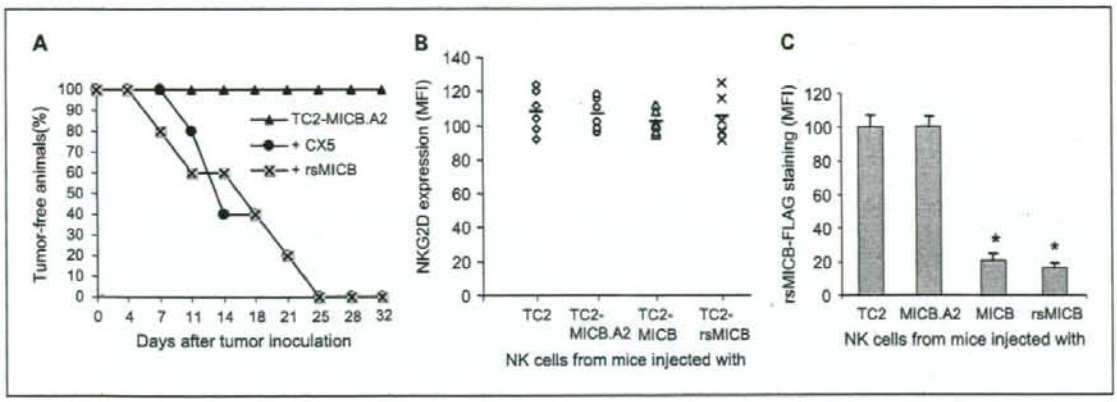

Fig. 6. Soluble MICB-induced NK cell dysfunction. *A, in vivo* blocking NKG2D with CX5 antibody or neutralization the function of NKG2D with rsMICB enables TC2-MICB.A2 cells to form tumors. To block NKG2D receptor *in vivo*, 100 μg NKG2D-specific antibody CX5 was injected intraperitoneally on the day before and the day after tumor implantation and thereafter every 3 d. To modify NKG2D function, animals were intraperitoneally injected with 50 ng purified rsMICB before implantation of TC2-MICB.A2 cells and thereafter twice a week for 4 wk. *B*, measurements of NKG2D expression shown as mean fluorescence intensity on splenic NK cells freshly isolated from SCID animals ($n = 6$) injected with various tumor cells. *Columns*, mean fluorescence intensity. *C*, competitive binding assay indicating saturation of NKG2D receptor by soluble MICB in animals bearing TC2-MICB and TC2-rsMICB tumors. Freshly isolated splenocytes were incubated with 10 ng/μL rsMICB-FLAG followed by FITC-conjugated anti-FLAG mAb M2 and PE-conjugated mAb DX5. Data are measurements of mean fluorescence intensity of M2 staining from six animals of each experimental group. *Bars*, SE. *, $P < 0.01$, compared with animals injected with TC2 or TC2-MICB.A2 tumor cells.

this study, although TC2 cells express some levels of mouse NKG2D ligand RAE-1 variants, TC2 tumors were palpable in SCID mice within 1 week after implantation and grew aggressively (Fig. 4), suggesting that the levels of activating RAE-1 variants expressed by TC2 cells are too low to induce antitumor immunity. This was also supported by the low binding ability of soluble mouse NKG2D to TC2 cells (Fig. 3A). Therefore, it could be challenging to define an optimal level of mouse NKG2D ligand expression for tumor rejection. Together, the choice of MICB makes the *in vivo* study described here more clinically relevant to human cancers.

In activated mouse NK cells, due to alternative DNA splicing, two isoforms of NKG2D couple with two intracellular adaptors, DAP10 and DAP12, which trigger phosphatidylinositol 3-kinase and Syk family protein tyrosine kinase, respectively (40, 41). In human, NKG2D only associates with DAP10. However, in mouse NK cells lacking DAP12 or Syk family kinases, DAP10-phosphatidylinositol 3-kinase pathway alone is sufficient to initiate ligand-induced NKG2D-mediated killing of target cells (41). Thus, regardless that signaling via mouse NKG2D is more complex than human NKG2D, effect of NKG2D ligand shedding on tumor formation as found in the current study would be significant in both species.

Most of the *in vitro* evidence suggests that engagement of tumor cell surface MIC to NKG2D can activate NK cell immunity against tumor cells. Thus, expression of MIC on tumor cells is proposed to activate host protective antitumor immunoresponse. However, most of the epithelial originated human cancer cells were found to have MIC expressed on the surface, suggesting the ineptness of MIC-induced NK cell immunity. Consistent with clinical observations, we also show that overexpressing the natural cleavable form of MICB in TC2 cells has no significant effect on tumor growth *in vivo*. Although overexpressing the noncleavable shedding-resistant MICB.A2 can cause TC2 tumor rejection, this effect can be inhibited by the persistent presence of soluble MICB (Fig. 6A). Together, our data suggest that the role of MIC in host tumor immunosurveillance is determined by whether MIC is all or partially membrane-bound. If all the MIC molecules sustain to be membrane-bound and noncleavable, expression of MIC activates NK cell-mediated host immunity. In contrast, if a portion of the MIC molecules is cleaved and becomes soluble, tumor cells cannot be targeted by NK cells due to soluble MIC-mediated masking and possible down-regulation of the receptor NKG2D regardless of abundant MIC remaining on the tumor cell surface as observed in many cancer patients (10–13).

In summary, our data provide the first *in vivo* conclusive evidence of the effect of MIC shedding on tumor growth and the importance of sustained MIC ligand-NKG2D receptor interaction in control of tumor growth. In addition, our results show no significant difference in tumor growth among animals whether the natural form of MICB or soluble recombinant MICB was expressed. This observation implies that wild-type MIC expression in established tumors may have very little effect on inducing host NK cell activation due to shedding of MIC by tumor cells and the consequent dampening of host immunity. Together, our results suggest that strategies to sustain the recognition of NKG2D receptor and tumor MIC ligand may have potential anticancer therapeutic implications.

Disclosure of Potential Conflicts of Interest

No potential conflicts of interest were disclosed.

Acknowledgments

We thank Michael Tao for assistance with animal tissue collections and Dr. Norman M. Greenberg for helpful discussions.

References

1. Cerwenka A, Bakker AB, McClanahan T, et al. Retinoic acid early inducible genes define a ligand family for the activating NKG2D receptor in mice. Immunity 2000; 12:721–7.
2. Diefenbach A, Jensen ER, Jamieson AM, Raulet DH. Rae1 and H60 ligands of the NKG2D receptor stimulate tumour immunity. Nature 2001;413:165–71.
3. Cerwenka A, Baron JL, Lanier LL. Ectopic expression of retinoic acid early inducible-1 gene (RAE-1) permits natural killer cell-mediated rejection of a MHC class I-bearing tumor *in vivo*. Proc Natl Acad Sci U S A 2001; 98:11521–6.
4. Diefenbach A, Hsia JK, Hsiung MY, Raulet DH. A novel ligand for the NKG2D receptor activates NK cells and macrophages and induces tumor immunity. Eur J Immunol 2003;33:381–91.
5. Carayannopoulos LN, Naidenko OV, Fremont DH, Yokoyama WM. Cutting edge: murine UL16-binding protein-like transcript 1: a newly described transcript encoding a high-affinity ligand for murine NKG2D. J Immunol 2002;169:4079–83.
6. Smyth MJ, Swann J, Cretney E, Zerafa N, Yokoyama WM, Hayakawa Y. NKG2D function protects the host from tumor initiation. J Exp Med 2005;202:583–8.
7. Long EO. Tumor cell recognition by natural killer cells. Semin Cancer Biol 2002;12:57–61.
8. Raulet DH. Roles of the NKG2D immunoreceptor and its ligands. Nat Rev Immunol 2003;3:781–90.
9. Cerwenka A, Lanier LL. NKG2D ligands: unconventional MHC class I-like-molecules exploited by viruses and cancer. Tissue Antigens 2003;61:335–43.
10. Groh V, Rhinehart R, Secrist H, Bauer S, Grabstein KH, Spies T. Broad tumor-associated expression and recognition by tumor-derived γδ T cells of MICA and MICB. Proc Natl Acad Sci U S A 1999;96:6879–84.
11. Vetter CS, Groh V, thor Straten P, Spies T, Brocker EB, Becker JC. Expression of stress-induced MHC class I related chain molecules on human melanoma. J Invest Dermatol 2002;118:600–5.
12. Jinushi M, Takehara T, Tatsumi T, et al. Expression and role of MICA and MICB in human hepatocellular carcinomas and their regulation by retinoic acid. Int J Cancer 2003;104:354–61.
13. Wu JD, Higgins LM, Steinle A, Cosman D, Haugk K, Plymate SR. Prevalent expression of the immunostimulatory MHC class I chain-related molecule is counteracted by shedding in prostate cancer. J Clin Invest 2004;114:560–8.
14. Friese MA, Platten M, Lutz SZ, et al. MICA/NKG2D-mediated immunogene therapy of experimental gliomas. Cancer Res 2003;63:8996–9006.
15. Busche A, Goldmann T, Naumann U, Steinle A, Brandau S. Natural killer cell-mediated rejection of experimental human lung cancer by genetic overexpression of major histocompatibility complex class I chain-related gene A. Hum Gene Ther 2006;17: 135–46.
16. Groh V, Wu J, Yee C, Spies T. Tumour-derived soluble MIC ligands impair expression of NKG2D and T-cell activation. Nature 2002;419:734–8.
17. Doubrovina ES, Doubrovin MM, Vider E, et al. Evasion from NK cell immunity by MHC class I chain-related molecules expressing colon adenocarcinoma. J Immunol 2003;171:6891–9.
18. Raffaghello L, Prigione I, Airoldi I, et al. Downregulation and/or release of NKG2D ligands as immune evasion strategy of human neuroblastoma. Neoplasia 2004;6:558–68.
19. Salih HR, Rammensee HG, Steinle A. Cutting edge: down-regulation of MICA on human tumors by proteolytic shedding. J Immunol 2002;169: 4098–102.
20. Holdenrieder S, Stieber P, Peterfi A, Nagel D, Steinle A, Salih HR. Soluble MICA in malignant diseases. Int J Cancer 2006;118:684–7.
21. Marten A, von Lilienfeld-Toal M, Buchler MW, Schmidt J. Soluble MIC is elevated in the serum of patients with pancreatic carcinoma diminishing γδ T cell cytotoxicity. Int J Cancer 2006;119:2359–65.
22. Diefenbach A, Jamieson AM, Liu SD, Shastri N, Raulet DH. Ligands for the murine NKG2D receptor: expression by tumor cells and activation of NK cells and macrophages. Nat Immunol 2000;1:119–26.
23. Dunn C, Chalupny NJ, Sutherland CL, et al. Human cytomegalovirus glycoprotein UL16 causes intracellular sequestration of NKG2D ligands, protecting against natural killer cell cytotoxicity. J Exp Med 2003;197:1427–39.
24. Li P, Morris DL, Willcox BE, Steinle A, Spies T, Strong RK. Complex structure of the activating immunoreceptor NKG2D and its MHC class I-like ligand MICA. Nat Immunol 2001;2:443–51.
25. Holmes MA, Li P, Petersdorf EW, Strong RK. Structural studies of allelic diversity of the MHC class I homolog MIC-B, a stress-inducible ligand for the activating immunoreceptor NKG2D. J Immunol 2002; 169:1395–400.
26. Strong RK. Asymmetric ligand recognition by the activating natural killer cell receptor NKG2D, a symmetric homodimer. Mol Immunol 2002;38: 1029–37.
27. Foster BA, Gingrich JR, Kwon ED, Madias C, Greenberg NM. Characterization of prostatic epithelial cell lines derived from transgenic adenocarcinoma of the mouse prostate (TRAMP) model. Cancer Res 1997;57:3325–30.
28. Bahram S, Spies T. Nucleotide sequence of a human MHC class I MICB cDNA. Immunogenetics 1996;43: 230–3.
29. Horton RM, Cai ZL, Ho SN, Pease LR. Gene splicing by overlap extension: tailor-made genes using the polymerase chain reaction. Biotechniques 1990;8: 528–35.
30. Ho EL, Carayannopoulos LN, Poursine-Laurent J, et al. Costimulation of multiple NK cell activation receptors by NKG2D. J Immunol 2002;169:3667–75.
31. Masuda H, Saeki Y, Nomura M, et al. High levels of RAE-1 isoforms on mouse tumor cell lines assessed by anti-"pan" RAE-1 antibody confer tumor susceptibility to NK cells. Biochem Biophys Res Commun 2002; 290:140–5.
32. Salih HR, Goehlsdorf D, Steinle A. Release of MICB molecules by tumor cells: mechanism and soluble MICB in sera of cancer patients. Hum Immunol 2006; 67:188–95.
33. Kaiser BK, Yim D, Chow IT, et al. Disulphide-isomerase-enabled shedding of tumour-associated NKG2D ligands. Nature 2007;447:482–6.
34. Wu J, Chalupny NJ, Manley TJ, Riddell SR, Cosman D, Spies T. Intracellular retention of the MHC class I-related chain B ligand of NKG2D by the human cytomegalovirus UL16 glycoprotein. J Immunol 2003;170:4196–200.
35. Ogasawara K, Hamerman JA, Hsin H, et al. Impairment of NK cell function by NKG2D modulation in NOD mice. Immunity 2003;18:41–51.
36. Diefenbach A, Raulet DH. The innate immune response to tumors and its role in the induction of T-cell immunity. Immunol Rev 2002;188:9–21.
37. Grossmann ME, Wood M, Celis E. Expression, specificity and immunotherapy potential of prostate-associated genes in murine cell lines. World J Urol 2001;19:365–70.
38. Le Maux Chansac B, Misse D, Richon C, et al. Potentiation of NK cell-mediated cytotoxicity in human lung adenocarcinoma: role of NKG2D-dependent pathway. Int Immunol 2008;20:801–10.
39. Gasser S, Orsulic S, Brown EJ, Raulet DH. The DNA damage pathway regulates innate immune system ligands of the NKG2D receptor. Nature 2005;436: 1186–90.
40. Diefenbach A, Tomasello E, Lucas M, et al. Selective associations with signaling proteins determine stimulatory versus costimulatory activity of NKG2D. Nat Immunol 2002;3:1142–9.
41. Zompi S, Hamerman JA, Ogasawara K, et al. NKG2D triggers cytotoxicity in mouse NK cells lacking DAP12 or Syk family kinases. Nat Immunol 2003;4: 565–72.